NEW MEXICO INSTITUTE OF MINING AND TECHNOLOGY

VISCOUS-MODEL STUDY OF GROUND WATER FLOW IN A WEDGE-SHAPED AQUIFER

by

DENNIS E. WILLIAMS

Submitted to the faculty of the
New Mexico Institute of Mining and Technology
in partial fulfillment of the requirements for
the degree of Master of Science
in Ground Water Hydrology

June, 1965

ACKNOWLEDGEMENT

The writer is grateful to Dr. Mahdi S. Hantush and Dr. Gerardo Wolfgang Gross of the New Mexico Institute of Mining and Technology for their valuable assistance while serving as thesis advisors. My appreciation also goes to Mr. L. A. Shaw of the Shell Oil Co. who kindly supplied the oil, dye, and helpful data.

Thanks are also extended to Mrs. Paula B. Bish who typed the material.

ABSTRACT

Analytical expressions are available which describe the average head distribution in artesian aquifers of non-uniform thickness. The expressions developed include both the steady and the unsteady-state cases. In these equations, the primary assumptions in addition to the homogeneity and uniformity of the hydraulic properties of the aquifer are that the slopes of the confining beds be less than 0.20, and that the flow lines be mainly horizontal. This flow problem is studied in a viscous-flow model in which two-dimensional flow is simulated. The experimental results, in general, show good agreement with the theoretical equations based on the above approximations.

CONTENTS

FIGURES

TABLES

PLATES

VISCOUS MODEL STUDY OF GROUND-WATER FLOW IN A WEDGE-SHAPED AQUIFER

INTRODUCTION

General

The flow of ground water in artesian aquifers of uniform thickness has been studied quite extensively. More common, however, is the flow of ground water in sands of nonuniform thickness, or more specifically, flow of ground water in sands whose thickness varies linearly (or approximately so) in the x-direction while remaining constant in the y-direction.

The flow of ground water between two parallel reservoirs connected by a wedge-shaped aquifer is a common occurrence, (see Fig. 1), as are the cases of converging or diverging sands draining surface reservoirs.

The head distribution in wedge-shaped aquifers is a function of the hydraulic properties of the aquifer as well as of the slope and of the inlet thickness. The flow in wedge-shaped aquifers cannot be approximated by the flow in aquifers of uniform thickness except during very short periods.

Previous Work

Analytical studies on the flow of ground water in sands of nonuniform thickness have been made by Hantush (1962). Approximate differential equations have been set up and solved for several problems of ground water flow in an aquifer in which the thickness varies

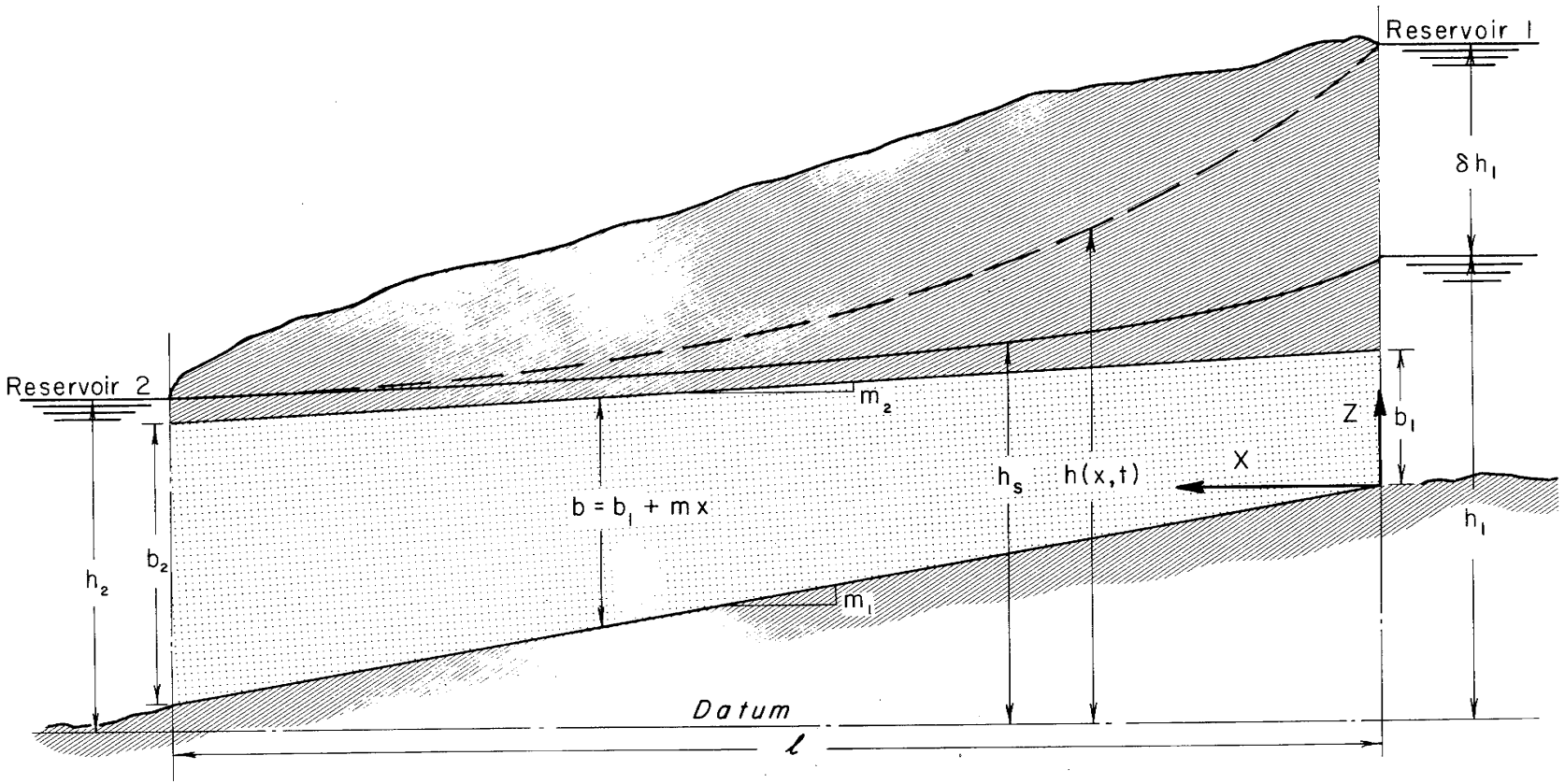

Fig. 1. Diagrammatic representation of a wedge-shaped aquifer connecting two parallel reservoirs

linearly or exponentially in the x-direction while remaining constant in the y-direction. Formulas for ground water flow have been obtained for several flow systems of practical interest. It is assumed in Hantush's work that the flow has no significant component of velocity in the y-direction so that its pattern is the same in all vertical (x-z) planes. The analytical results he obtained are presented in terms of functions that are available in tabular form, thus making these analytical expressions as easy to use as any other formulas.

Purpose of Study

The primary assumption in Hantush's work is that the flow lines in such wedge-shaped aquifers will be mainly horizontal when the slopes of the confining beds are less than 0.20. The assumption appears logical. Its validity, however, has not been tested against experimental data.

The purpose of the present study is to test the theoretical equations against experimental results using a viscous-flow model for the following cases:

(1) Steady flow in a wedge-shaped aquifer connecting two surface reservoirs, with the flow in the direction of divergence and convergence.

(2) Unsteady flow in a semi-infinite, wedge-shaped aquifer diverging linearly in the direction of flow. In this case the model does not reproduce the prototype exactly.

(3) The experimental data of unsteady flow in a semi-infinite, linearly converging aquifer will be compared with the theo-

retical solution based on an aquifer that thins out exponentially.

THEORY

Basic Considerations

Figure 1 shows a cross section of a wedge-shaped aquifer connecting two parallel, surface reservoirs. The aquifer is confined between two impermeable strata, whose angles of dip have tangents not greater than 0.20. The aquifer is of infinite areal extent. The water-bearing material is sand of uniform hydraulic conductivity K and uniform specific storage S_s. The head observed in a hole (or screened well) completely penetrating the sand reflects the average head along the sand profile cut by the hole. The numerical values of the slopes (m_1 and m_2) will be positive or negative depending on whether the confining bed is sloping upward or downward in the direction of positive x. The z-coordinate is positive upward and the lower confining bed passes through the origin of coordinates.

Notation

The major symbols in this presentation are identified where they first appear and are listed alphabetically in Appendix III.

Method of Analysis

Figure 1 shows a wedge-shaped aquifer connecting two surface reservoirs of height h_1 and h_2, and separated by a distance ℓ. The inlet and outlet thicknesses are b_1 and b_2, respectively, and the slopes of the confining beds are m_1 and m_2.

The height of the steady-state profile is represented by h_s. If we now consider the aquifer to be semi-infinite (that is to say, if we disregard reservoir 2) and if we suddenly change the head on reservoir 1 by an amount δh_1 and keep it constant thereafter, then the profile of the head at any time and distance will be given by $h(x,t)$.

Consider the sketches in figures 9, 10, and 11 of a linearly pinching-out aquifer. If the head of the reservoir is initially at h_i and suddenly changed to h_1 and held constant thereafter, then the resulting head distribution at any time and distance may be approximated by a solution based on a semi-infinite sand thinning out exponentially, and is also designated $h(x,t)$.

Analysis

The flow of ground water is described by the following differential equation (Jacob, 1950):

$$\frac{\partial v_x}{\partial x} + \frac{\partial v_y}{\partial y} + \frac{\partial v_z}{\partial z} = - S_s \frac{\partial \phi}{\partial t} \qquad (1)$$

where ϕ is the piezometric (hydraulic) head v_x, v_y, v_z are bulk velocities in the respective directions, and S_s is the specific storage of the aquifer.

If the average head, mentioned on page 5, obeys Darcy's law then:

$$V_x = - K \, \partial h/\partial x$$
$$V_y = - K \, \partial h/\partial y \qquad (2)$$

Now integrating (1) with respect to z in a vertical line where the

aquifer thickness is equal to $b(x,y) = f_2 - f_1$, where f_2 and f_1 equal the value of z at the upper and lower boundaries respectively, we obtain:

$$\int_{f_1}^{f_2} \frac{\partial v_x}{\partial x}\, dz + \int_{f_1}^{f_2} \frac{\partial v_y}{\partial y}\, dz + \int_{f_1}^{f_2} \frac{\partial v_z}{\partial z}\, dz = - S_s \int_{f_1}^{f_2} \frac{\partial \phi}{\partial t}\, dz \qquad (3)$$

Making use of Leibnitz's rule of differentiation under the integral sign and remembering that v_x and v_y are functions of (x,y,z,t) and that f_1 and f_2 are functions of x and y, we can put (3) in the form of:

$$\frac{\partial}{\partial x}\left[\int_{f_1}^{f_2} v_x\, dz\right] - v_x(x,y,f_2,t)\, \frac{\partial f_2}{\partial x} + v_x(x,y,f_1,t)\, \frac{\partial f_1}{\partial x}$$

$$+ \frac{\partial}{\partial y}\left[\int_{f_1}^{f_2} v_y\, dz\right] - v_y(x,y,f_2,t)\, \frac{\partial f_2}{\partial y} + v_y(x,y,f_1,t)\, \frac{\partial f_1}{\partial y} \qquad (4)$$

$$+ v_z(x,y,f_2,t) - v_z(x,y,f_1,t) = - S_s \frac{\partial}{\partial t}\left[\int_{f_1}^{f_2} \phi\, dz\right]$$

The bracketed quantities in (4) are readily recognized as bV_x, bV_y and

bh respectively. Since f_1 is a stream surface, the total velocity at any point in this surface must lie in the plane tangent to the surface. The same holds for f_2. From analytic geometry it can be shown that:

$$v_z(x,y,f_1,t) = v_x(x,y,f_1,t) \frac{\partial f_1}{\partial x} - v_y(x,y,f_1,t) \frac{\partial f_1}{\partial y}$$

Applying the same rule to f_2 and using the relations of (2) in conjunction with (4) we obtain:

$$\frac{\partial}{\partial x} b(x,y) \frac{\partial h}{\partial x} + \frac{\partial}{\partial y} b(x,y) \frac{\partial h}{\partial y} = \frac{b(x,y)}{\nu} \frac{\partial h}{\partial t} \qquad (5)$$

where $\nu = K/S_s$. Now if the thickness varies in the x-direction only, (5) reduces to:

$$\frac{\partial^2 h}{\partial x^2} + \frac{1}{b} \frac{\partial b}{\partial x} \frac{\partial h}{\partial x} + \frac{\partial^2 h}{\partial y^2} = \frac{1}{\nu} \frac{\partial h}{\partial t} \qquad (6)$$

which is the approximate differential equation of motion in sands of non-uniform thickness.

FLOW IN A SEMI-INFINITE WEDGE-SHAPED AQUIFER

Consider the flow system of figures 6, 7, and 8. An infinitely long channel along the y-axis completely cuts through a semi-infinite sand that thickens away from the channel in accordance with the relation:

$$b = f_2 - f_1 = (b_1 + m_2 x) - m_1 x = b_1 + mx \qquad (7)$$

If in the above flow system the initial head h_i is uniform everywhere and if the water level in the channel is suddenly changed from h_i to a new elevation h_1 and maintained constant thereafter, then the head distribution, as observed from (6) and (7), (Hantush, 1962) is given by:

$$h(x,t) = h_i + (h_1 - h_i)\ A\left(\frac{b_1 + mx}{b_1},\ \frac{\nu\, t\, m^2}{b_1^2}\right) \qquad (8)$$

where b_1 is the inlet thickness, $m_2 - m_1 = m$, and $A(x,t)$ is the flowing-well function (Hantush, 1964). This solution, based on the approximate differential equation, is equivalent to the rigorous solution established by Hantush (1962) if the slopes of the confining beds are less than 0.20.

STEADY-STATE FLOW BETWEEN TWO PARALLEL RESERVOIRS

Consider unidirectional flow (in the x-direction) in the wedge-shaped aquifer of figure 1. The aquifer thickness is uniform in the y-direction (normal to the plane of the paper) but varies linearly in the x-direction in accordance with (7).

The approximate steady-state equation describing the flow in this aquifer is, from (6) and (7):

$$\frac{\partial^2 h}{\partial x^2} + \frac{m}{b_1 + mx}\frac{\partial h}{\partial x} = 0 \qquad (9)$$

The solution which satisfies the two end conditions of constant head is (from Hantush, 1962):

$$h_s = h_1 - (h_1 - h_2) \frac{\ell n \left[(b_1 + mx)/b_1 \right]}{\ell n \left[(b_1 + m\ell)/b_1 \right]} \qquad (10)$$

If we rotate the system shown in figure 1 by 180°, geometrically it will be the same as the previous steady-state system but with the boundary conditions interchanged. Thus, we obtain the head distribution in the rotated system if we replace the parameters m, b_1, h_1, and x by - m, b_2, h_2, and ℓ - x respectively.

FLOW IN A SEMI-INFINITE SAND THINNING OUT EXPONENTIALLY

If the aquifer thickness is uniform in the y-direction but thins out in the positive x-direction according to the law:

$$b = b_1 \exp (- 2x/a) \qquad (11)$$

where "a" is a geometrical parameter defining the exponential variation of the aquifer thickness, then the approximate differential equation governing the unidirectional flow (in the x-direction) can be obtained from (6) and (11) as:

$$\frac{\partial^2 h}{\partial x^2} - \frac{2}{a} \frac{\partial h}{\partial x} = \frac{1}{\nu} \frac{\partial h}{\partial t} \qquad (12)$$

The validity of (12) and the solutions derived therefrom are assured if

$\left| \frac{\partial b}{\partial x} \right| < 0.20$ for all boundaries of x within the flow system

(Hantush, 1962).

If the water level in the channel is suddenly changed an amount δh_1 and kept constant thereafter, then the head distribution satisfying the given boundary conditions is given by Hantush, (1962) as:

$$h(x,t) = h_i + \frac{1}{2}\,\delta h_1 \left[\operatorname{erfc}\left(\frac{x}{\sqrt{4\nu t}} - \frac{\sqrt{\nu t}}{a} \right) + \right. \tag{13}$$

$$\left. + \exp(2x/a)\, \operatorname{erfc}\left(\frac{x}{\sqrt{4\nu t}} + \frac{\sqrt{\nu t}}{a} \right) \right]$$

The value of the parameter "a" for the exponentially varying thickness is obtained by equating the area of the triangular section of the wedge-shaped aquifer to that of the exponentially varying section, which is assumed to extend to infinity (see inserts in figures 9, 10, and 11). This value of "a" is equal to b_1/m.

MODEL STUDIES

Model Analogy

The analogy between ground-water flow and viscous flow in models is based on the similarity between the differential form of Darcy's law and Poiseuille's equation (Bear, 1960), and, further, on the similarity between the differential equations which describe the saturated-flow field in porous media, and those which describe the laminar flow of viscous fluids in a capillary spacing between two parallel plates.

Darcy's law describes the saturated flow of ground water provided that the flow is laminar, that is, if the velocity of flow is proportional to the first power of the hydraulic gradient. The generalized form of Darcy's law is expressed by Jacob (1950) as:

$$v = - K \frac{\partial \phi}{\partial s} \tag{14}$$

where v is the bulk velocity in the direction of s at any point in the field of flow, and the other terms have already been defined.

The flow between two parallel plates obeys Poiseuille's equation which is given by Bear (1960) as:

$$v_m = -(1/12) \left[g \left(b_m^2 / \nu_f \right) \right] \frac{dh}{ds} \tag{15}$$

where v_m is the average velocity of the fluid at a point (x,z) in the model; ν_f is the kinematic viscosity of the fluid (see Appendix II); b_m is the spacing between the plates; g is the acceleration due to gravity; and s is the length along the direction of flow.

Poiseuille's equation (15) can be written as:

$$v_m = - K_m \frac{dh}{ds} \tag{16}$$

where

$$K_m = \left(1/12\right) g \frac{b_m^2}{\nu_f} \tag{17}$$

may be thought of as the hydraulic conductivity of the model aquifer.

Poiseuille's law, which describes the flow in the model, is given in terms of the average of the velocity distribution between the two plates. The bulk velocity of ground water in the prototype (natural aquifer), is also given as an average velocity. Thus, if these velocities are compared, a kinematic similarity exists. Since the flow in the prototype and in the model have similar mass distributions, the criterion is thus established for dynamic similarity.

The two-dimensional differential equation of ground water flow in an anisotropic aquifer is given by Jacob (1950) as:

$$K_{xp} \frac{\partial^2 h_p}{\partial x_p^2} + K_{zp} \frac{\partial^2 h_p}{\partial z_p^2} = S_{sp} \frac{\partial h_p}{\partial t_p} \tag{18}$$

where p is a subscript denoting prototype.

The two-dimensional differential equation for the viscous flow in a capillary interspace between two vertical parallel plates has been shown by Bear (1960) to be:

$$K_{xm} \frac{\partial^2 h_m}{\partial x_m^2} + K_{zm} \frac{\partial^2 h_m}{\partial z_m^2} = S_{sm} \frac{\partial h_m}{\partial t_m} \qquad (19)$$

where m is a subscript denoting model. Thus, the same differential equations describe model and prototype flows. However, viscous-flow models describe the flow in isotropic media so that:

$$K_{xm} = K_{zm} = K_m \qquad (20)$$

Bear (1960) gives a detailed and rigorous analysis of the mathematical similitude.

Model Scales

The relations between the model and the prototype are obtained as follows:

$$\begin{aligned} K_{xp} &= \frac{K_{xm}}{R_{K_x}} \quad ; \quad K_{zp} = \frac{K_{zm}}{R_{K_z}} \\ x_p &= \frac{x_m}{R_x} \quad ; \quad z_p = \frac{z_m}{R_z} \\ h_p &= \frac{h_m}{R_h} \quad ; \quad S_{sp} = \frac{S_{sm}}{R_{S_s}} \\ t_p &= \frac{t_m}{R_t} \end{aligned} \qquad (21)$$

Where R denotes model-prototype ratio.

By noting relation (20) and substituting equations (21) into equation (18) one obtains the equation as follows:

$$\frac{K_m \, \partial^2\left(\frac{h_m}{R_h}\right)}{R_{K_x} \, \partial\left(\frac{x_m}{R_x}\right)^2} + \frac{K_m \, \partial^2\left(\frac{h_m}{R_h}\right)}{R_{K_z} \, \partial\left(\frac{z_m}{R_z}\right)^2} = \frac{S_{sm} \, \partial\left(\frac{h_m}{R_h}\right)}{R_{S_s} \, \partial\left(\frac{t_m}{R_t}\right)} \qquad (22)$$

rearranging equation (22) results in:

$$\frac{R_x^2}{R_{K_x} R_h} K_m \frac{\partial^2 h_m}{\partial x_m^2} + \frac{R_z^2}{R_{K_z} R_h} K_m \frac{\partial^2 h_m}{\partial z_m^2} = \frac{R_t}{R_{S_s} R_h} S_{sm} \frac{\partial h_m}{\partial t_m} \qquad (23)$$

If equation (23) is to reduce to equation (19) then the following relation will have to hold.

$$\frac{R_x^2}{R_{K_x} R_h} = \frac{R_z^2}{R_{K_z} R_h} = \frac{R_t}{R_{S_s} R_h} \qquad (24)$$

LENGTH SCALES

From equation (24) one immediately obtains:

$$\frac{R_x^2}{R_z^2} = \frac{R_{K_x}}{R_{K_z}}$$

and since $K_{xm} = K_{zm}$,

$$\frac{R_x^2}{R_z^2} = \frac{K_{xm} \, K_{zp}}{K_{xp} \, K_{zm}} = \frac{K_{zp}}{K_{xp}} \qquad (25)$$

Equation (25) describes the distortion in length scales in cases of anisotropic media. In the investigation of wedge-shaped aquifers, one would like to keep the angles of the confining beds the same from

model to prototype. To do this requires that $R_z = R_x$, and consequently, $K_{zp} = K_{xp}$. Thus, in angle-preserving modeling of wedge-shaped aquifers, the prototype sand must be isotropic.

TIME SCALE

From equation (24):

$$R_t = \frac{R_{S_s} R_x^2}{R_{K_x}^2} \tag{26}$$

and:

$$t_m = \frac{R_{S_s} R_x^2 K_{xp}}{K_m} t_p \tag{27}$$

Substituting the value of K_m from equation (17) into equation (27) yields:

$$t_m = \frac{12}{g} R_{S_s} K_{xp} \frac{R_x^2 \nu_f}{b_m^2} t_p \tag{28}$$

EXAMPLE OF SCALING

The following prototype aquifer has been constructed using actual field values for the formation parameters.

$K_p = 1 \times 10^{-4}$ ft/sec $\qquad K_m = 4.6 \times 10^{-3}$ ft/sec

$S_{sp} = 1.4 \times 10^{-3}$ ft^{-1} $\qquad S_{sm} = 1.9$ ft^{-1}

$b_{lp} = 60$ ft $\qquad b_{lm} = 0.23$ ft

$\ell p = 2083$ ft $\qquad \ell m = 8.1$ ft

For a sudden change in level of 30 ft in a stream, it is desired to find out the time required for this sudden change of head to be noticeable in a well located 2083 ft from the stream. The stream is drained by a wedge-shaped aquifer whose inlet thickness to the stream is 60 ft. The upper confining bed of the sand is horizontal, while the lower confining bed slopes downward away from the stream at an angle of 5°.

From eq. (25) one obtains the relations:

$$z_p = 260 z_m \quad ; \quad x_p = 260 x_m$$

From Eq. (28) one obtains:

$$t_p = 2210 t_m$$

The 30 ft change in head in the prototype sand corresponds to about a 3.5 cm change in head in the model aquifer. The time required to notice a change in level at the other end of the model aquifer is about 1 hour. From the above relation then, the time required to notice a change in water level in the well is about 92 days.

Model Characteristics

The viscous-flow or Hele-Shaw model is designed primarily to study a vertical two-dimensional flow field. The viscous analogy model is much to be preferred over the conventional sand model because the problems of channeling and entrapped air are not present. Since the model is transparent it is possible to inject dye and study the stream lines, as well as to observe visually the phreatic surface

or piezometric head as the case may be.

The hydraulic conductivity of the model aquifer depends upon the plate spacing, the kinematic viscosity of the fluid, and the acceleration of gravity. The hydraulic conductivity can be kept constant if the spacing and temperature are constant. This is another great advantage over sand models where uniform packing of the sand is extremely difficult to obtain.

Description of the Model

The viscous-flow model was first introduced by Professor Hele-Shaw in 1897 to study the nature of flow around obstructions of various shapes. Dachler (1936), Gunther (1940), Dietz (1941), Santing (1951), and Todd (1954) among others have used such models in their studies of flow through water-bearing materials. Figures 2 and 3 and Plates I through V show the model used in the present investigation.

The model consists of two Plexiglas(acrylic resin) plates, each 1.27 cm thick. The plates are 244 cm long and 30.5 cm high. The spacing between the plates is maintained by brass washers (see figure 3 and Plate V). The confining layer is simulated by medium durometer Neoprene, 0.16 cm thick, cut in strips, and a 5° wedge as shown in the illustrations. At each end of the plates is situated a rectangular reservoir. These reservoirs are connected to the aquifer by means of a block of Plexiglas, 1.9 cm thick, through which a slot, the depth of the aquifer, is cut in order to pass the fluid (see Plates). The model rests on a steel base, and is supported by 4 braces on the sides.

The specific storage of the aquifer was modeled by cutting slots

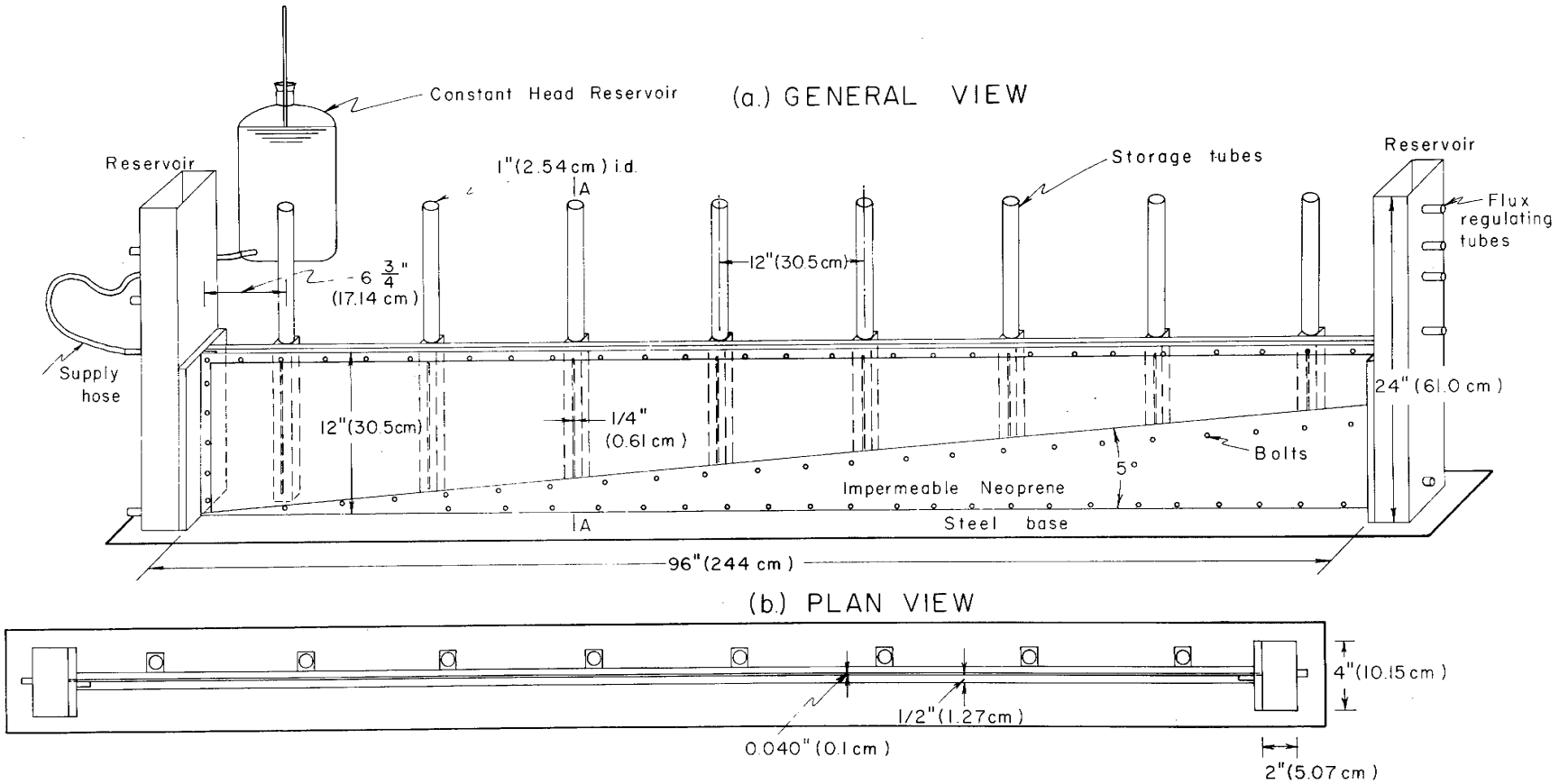

Note: Exact head piezometer tubes have been eliminated for sake of clarity (see Plates)

Fig. 2 Diagrams showing viscous flow model

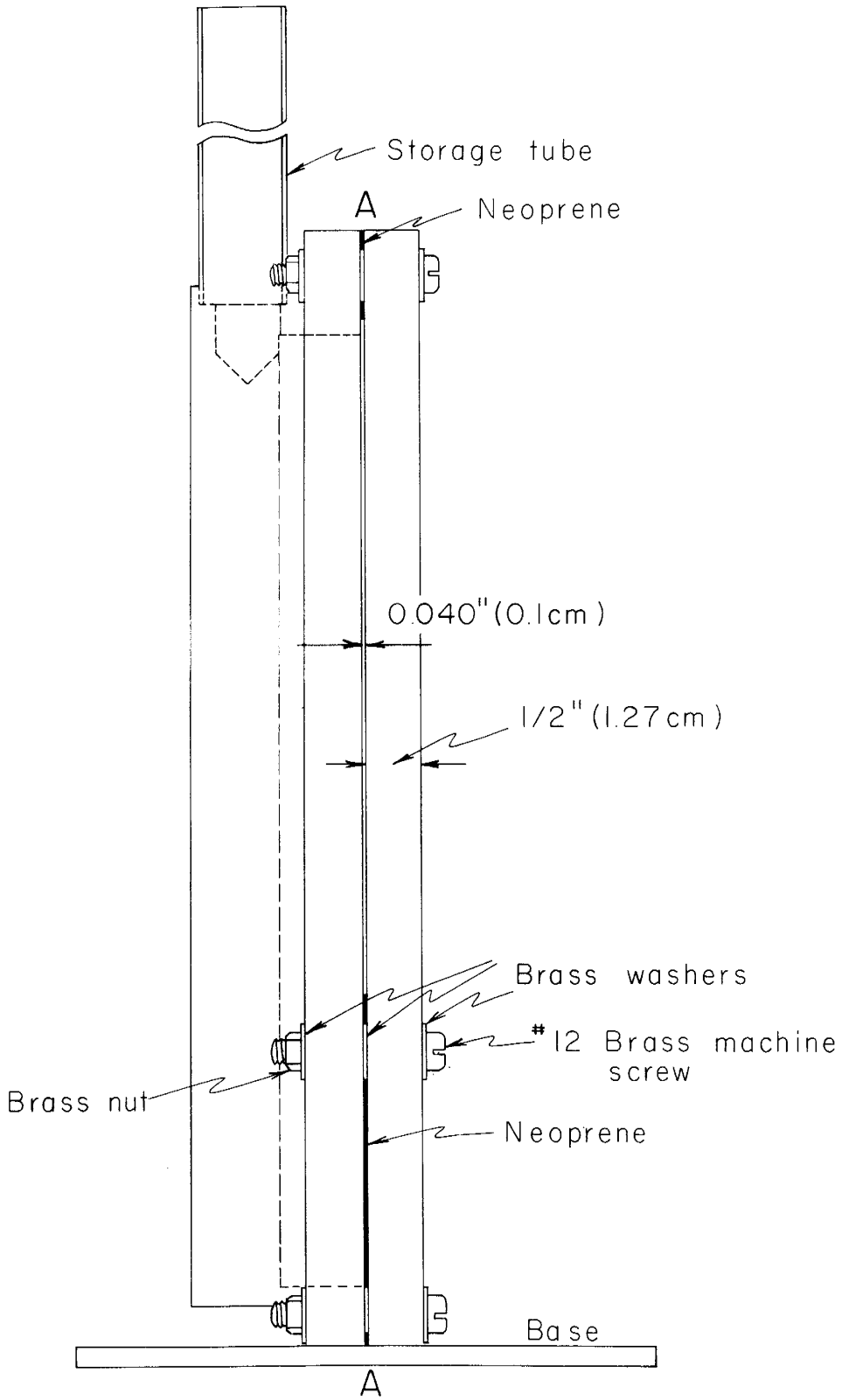

Fig. 3 Cross section through model

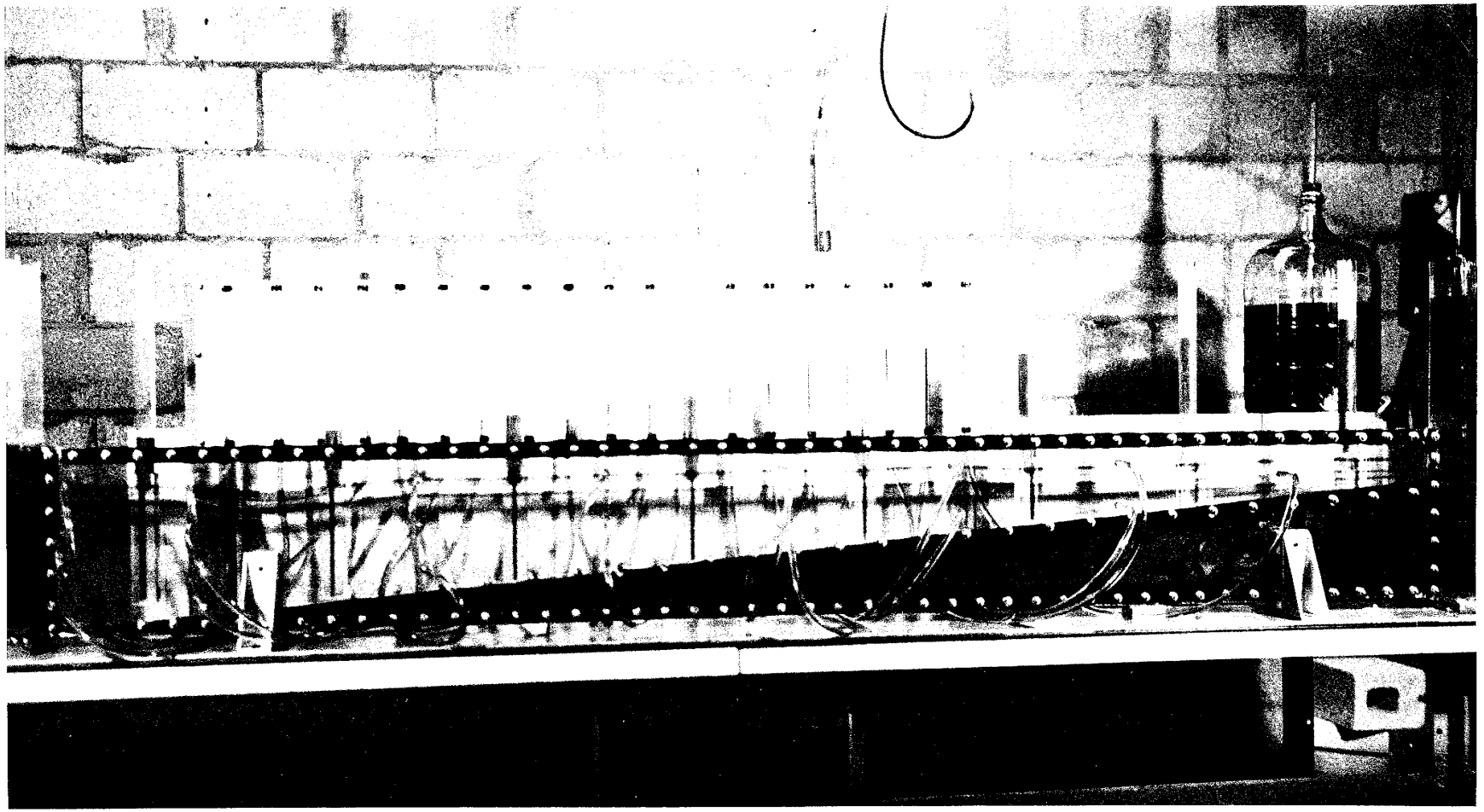

Plate I General view of the model showing flow lines

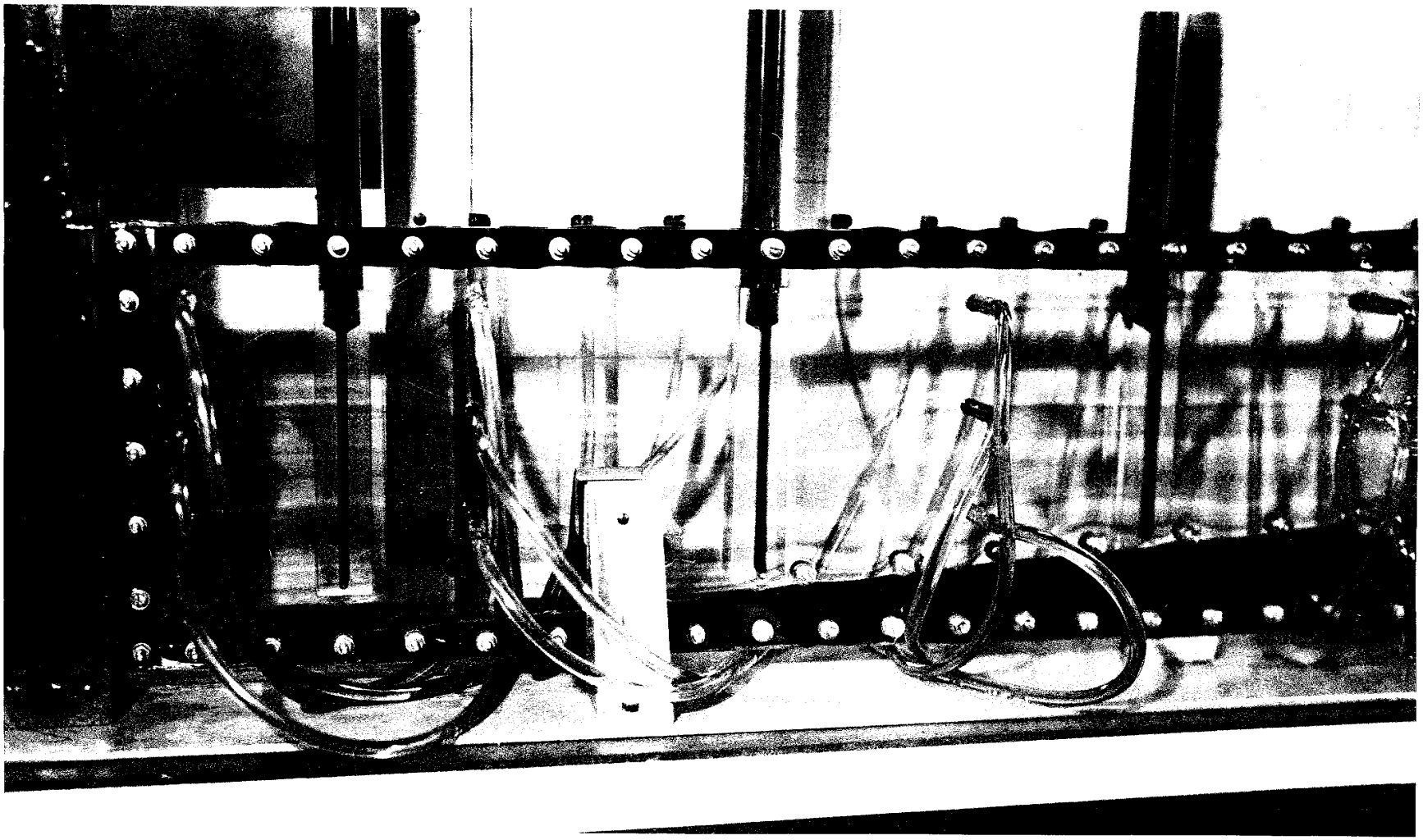

Plate II View of diverging end of model showing flow lines

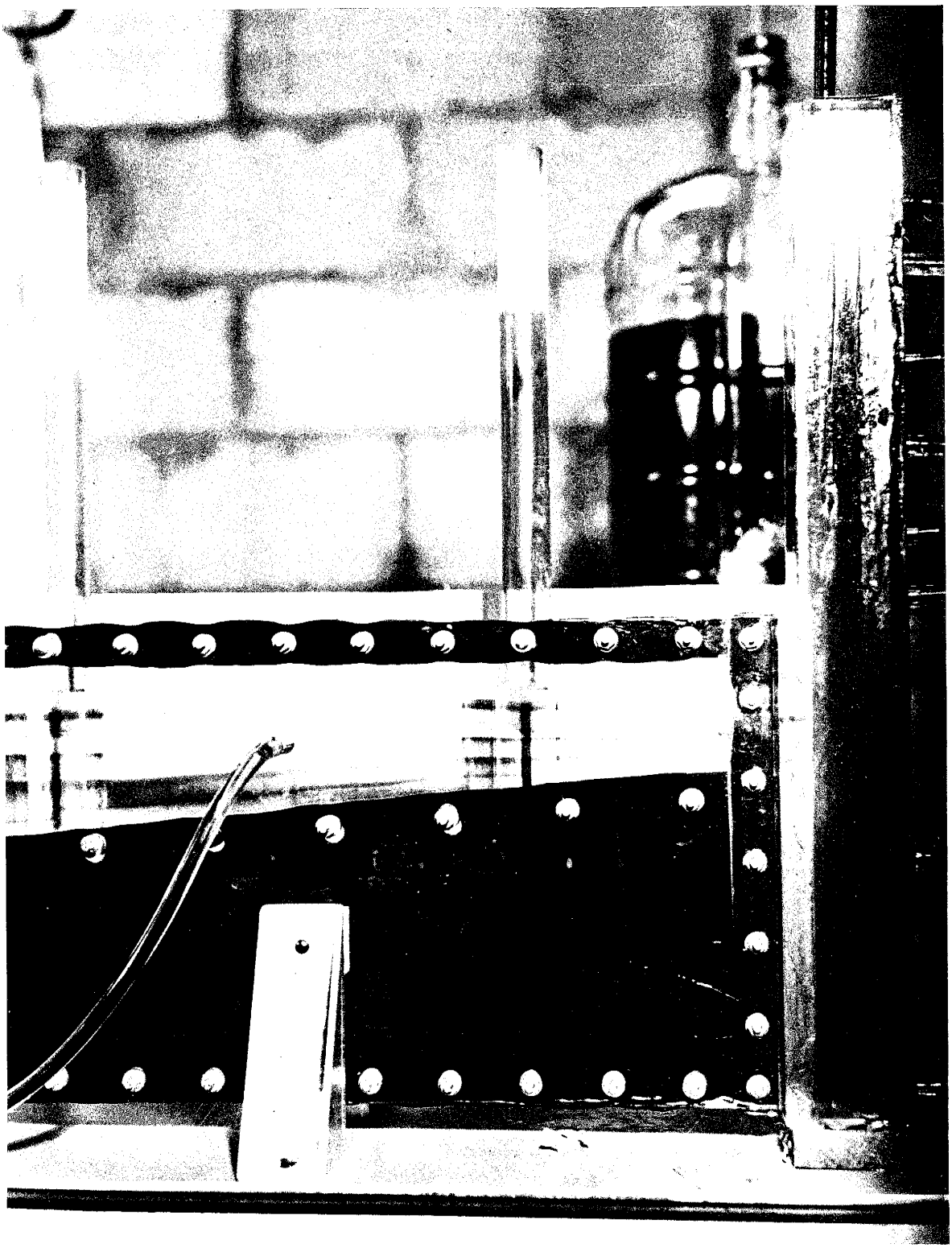

Plate III View of converging end of model showing flow lines

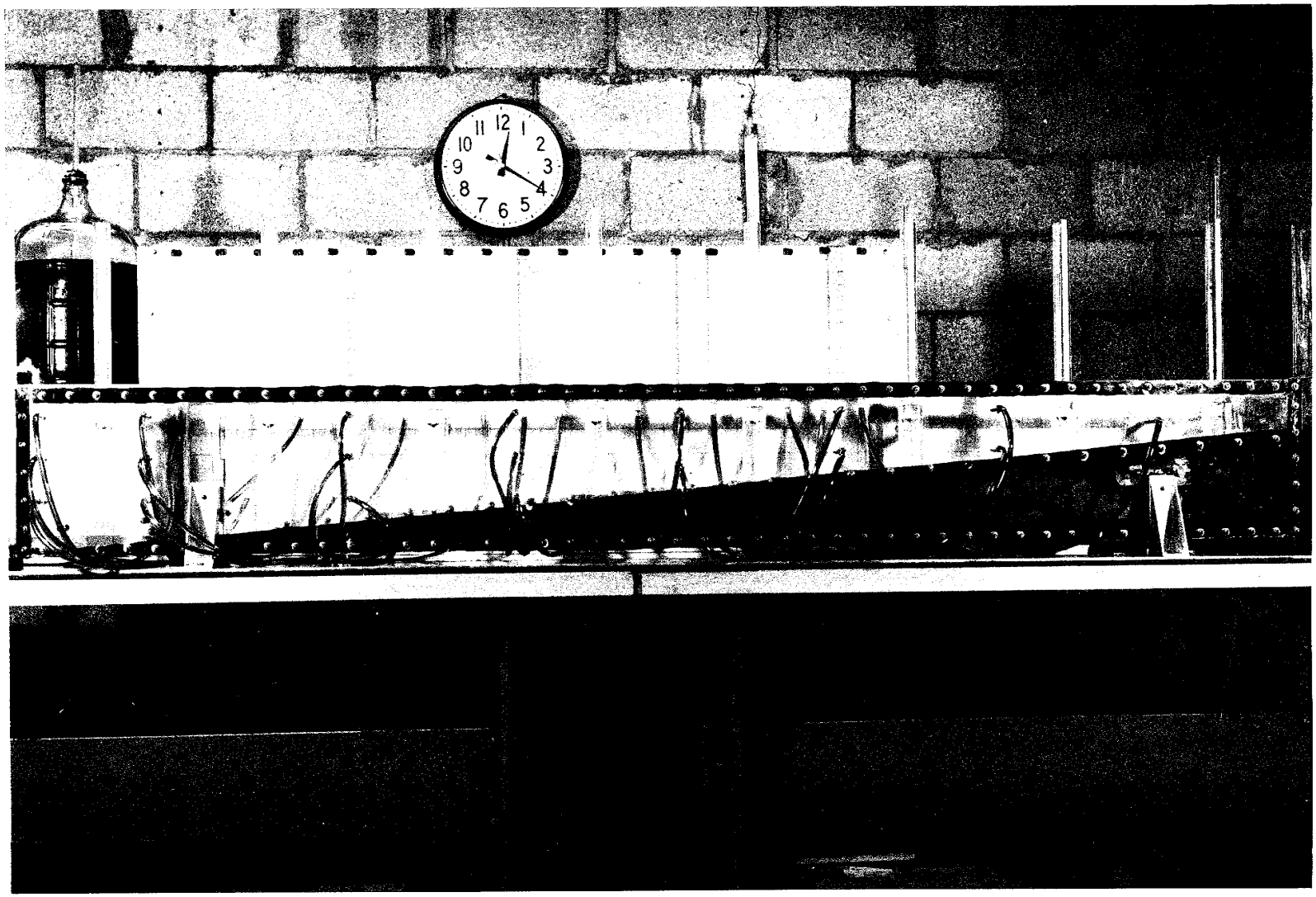

Plate IV View of model showing compensating rods inserted in the storage tubes

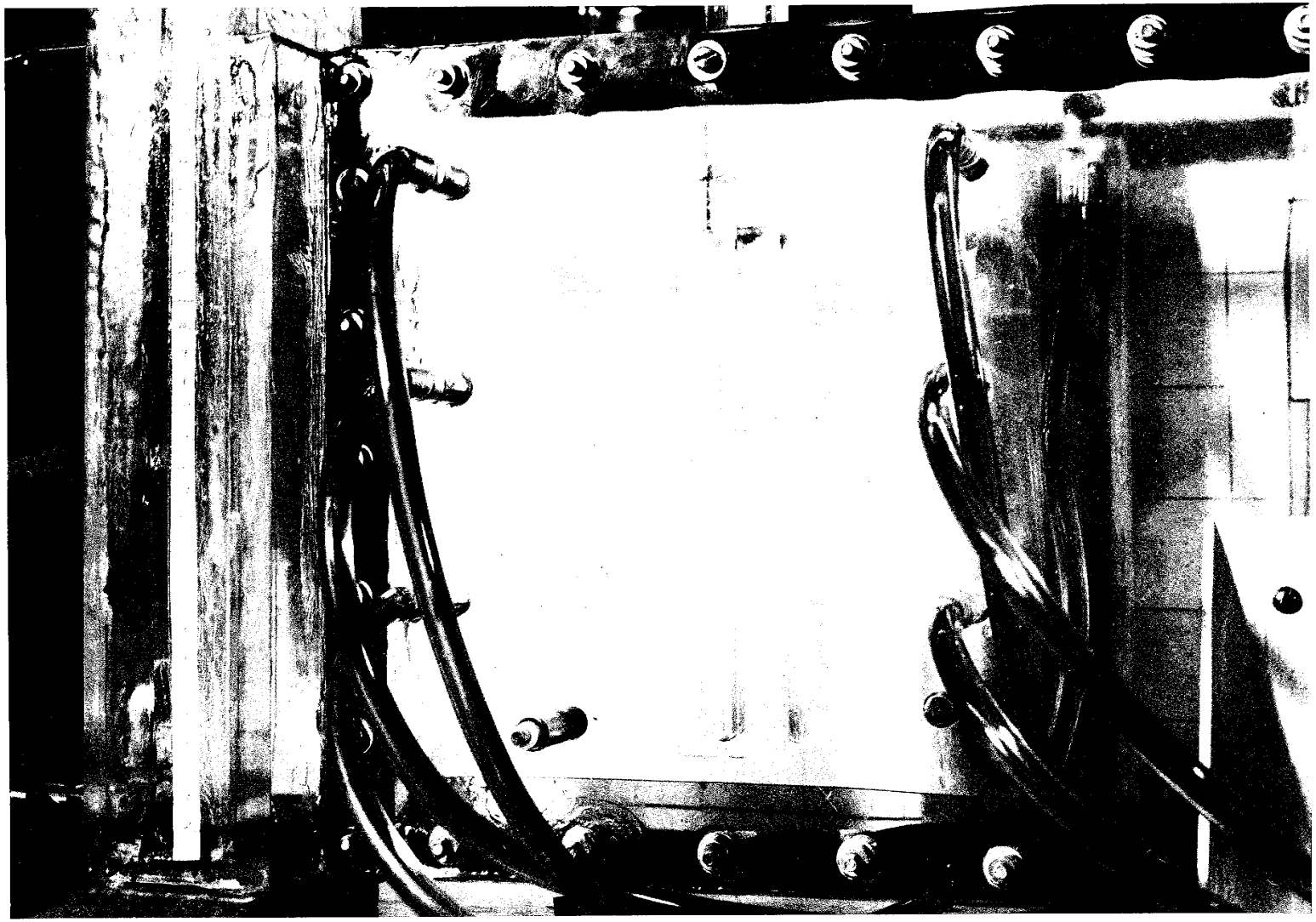

Plate V Close up of model showing details

in the back plate approximately equal to the depth of the aquifer. Over these slots were glued storage blocks into which tubes were inserted (see figures 2 and 3, and Plates II, III, and V).

Each storage tube is supposed to account for fluid taken into or out of storage in a 30.5 cm segment of the aquifer.

To keep the specific storage constant, or nearly so, throughout the aquifer, one must in turn decrease the diameter of the storage tubes in the direction of convergence. To accomplish this, Plexiglas rods of increasing diameter were inserted into the storage tubes in the direction of convergence (see Plate IV). For dimensions of these rods as well as of the effective storage tube area see Table V.

Tubes were also installed at specific points in the front plate to measure the exact hydraulic head at that point (see Plates). These tubes were then connected by Tygon tubing to piezometer tubes arrayed on a grid board. These piezometer tubes are to be used in future work.

A constant head could be maintained by use of a constant-head reservoir (Mariotte bottle), which was connected to the reservoirs at various places through the flux-regulating tubes (see figure 2).

Drains were situated at the bottom of the reservoirs to facilitate emptying. Flow lines were observed by injecting a red oil-base dye into the flow system (see Plates I, II, and III). This was accomplished by means of inserting into one reservoir a capillary tube with several small openings drilled in it. The capillary tube was in turn connected to a constant supply of dye.

The fluid was kept at a constant temperature of 70° Fahrenheit by means of a regulating thermostatic heater in the laboratory. Some

physical properties of the viscous fluid used are given in Appendix II.

EXPERIMENTAL PROCEDURE

Calibration of the Model

The plate spacing of the two dimensional viscous-flow model is calibrated by introducing a known volume of fluid between the plates. An accurate determination of this parameter is difficult to obtain because of the many unmeasurable volumes involved, such as storage tubes, piezometer tubes, slots, etc. Because of this, the spacing between the plates was accepted to be that of the brass spacing washers (0.1 cm). A small variation in plate spacing in this model is not critical as far as the final results are concerned, and at the most could contribute second-order errors.

Description of Experiments

The purpose of the experiments was to check the validity of equations (8) and (10) and to see if the head distribution in a linearly converging aquifer could be approximated by equation (13), the solution for a semi-infinite, exponentially decreasing aquifer. The main approximation in these equations is that the slopes of the confining beds be less than 0.20.

For steady-state runs, the head on one reservoir was maintained constant, through use of the constant-head bottle. The other reservoir was maintained constant at a lower level by means of an overflow tube.

For non-steady-state runs, the piezometric surface (storage tube levels) was first allowed to attain a uniform initial level.

Then the head in one reservoir was suddenly changed and kept constant. To keep the flow system semi-infinite, the experiment was terminated when the effect of the sudden change in head became noticeable at the far end of the aquifer (last storage tube).

Measurement Procedure

STEADY STATE

After the model was filled with oil and all air pockets expelled from between the plates, the head on each reservoir was maintained constant at different levels. This was accomplished by using the Mariotte bottle and an overflow tube. The head on the upper reservoir was determined by the height of the bottom of the air pipe in the Mariotte bottle. The model was left to flow for several hours until conditions of dynamic equilibrium (steady-state) existed. At this time, the averave hydraulic head, as seen in the storage tubes, was recorded. A millimeter strip glued on these tubes was used to measure the head.

UNSTEADY STATE

In this case the model was allowed to attain an initial horizontal level everywhere. Then at time zero, the head on one reservoir was suddenly changed to a new level by rapidly pouring the required volume in and at the same time opening a pinch clamp to the constant-head reservoir (Mariotte bottle). In this way a sudden and constant change in head was effected. Then at times 30, 60, 90, 120, 180, 300, 600, and 1200 seconds the average hydraulic head was observed and recorded. Thus, an average head profile of the aquifer at varying times was obtained. The experiment was terminated when a change in level

was observed in the last storage tube.

Probable Experimental Errors

OBSERVATION AND PROCEDURE ERRORS

Probable experimental errors in this investigation occur in: keeping the temperature constant from run to run; reading the height of the piezometric surface; and in making these readings at the prescribed time (in the unsteady cases). Although the temperature varied as much as 1 or 2 degrees throughout all the experiments, it is evident from figure 14 that this did not significantly affect the results. Another factor that may introduce experimental error is the requirement that the head change be instantaneous in the unsteady case. This requirement is satisfied, in these experiments, as the high viscosity of the oil allowed the desired instantaneous change without significant flow.

As previously stated, unsteady-state data were recorded for specified times. As it was impossible to read all 8 storage tubes simultaneously, an average of the time required to read all the tubes was used.

CONSTRUCTION AND MODELING ERRORS

Errors in construction and modeling seem to outweigh those discussed in the preceding section. For example, the plate spacing is not entirely constant, as evidenced by the flow lines. Some evidence of circulation in the storage tubes can also be observed by studying the flow lines. An examination of the Plates shows, however, that both the irregular spacing and the circulation have only small effects

on the streamlines (see Plates I, II, and III).

Probably the greatest experimental deviation is due to the improper spacing of the storage tubes.

There may also be some error introduced, due to the fact that, the slots in the back plate are not exactly equal to the depth of the aquifer, although approximately so.

PRESENTATION OF DATA AND DISCUSSION OF RESULTS

The observed and calculated data for steady-state conditions are given in Tables I and II. Table I is for the diverging case, and Table II is for the converging case. The calculated values for Tables I and II were obtained using equation (10) and the 180° rotation of (10) respectively.

A relative per-cent deviation was computed between the observed and calculated head. This was accomplished by taking the difference between the two values and dividing this difference by the difference between surface reservoir levels in the steady-state cases, and by the sudden change in head in the unsteady-state cases. This ratio was then multiplied by 100. These per-cent deviations in the steady-state cases ranged from 0.07% to 12.76%.

The unsteady-state data for a semi-infinite linearly diverging wedge-shaped aquifer are given in Table III. The calculated values were computed using equation (8). The per-cent relative deviation for these cases ranged from 0.00% to 14.23%.

Observed unsteady-state data for a semi-infinite linearly converging aquifer are given in Table IV. The calculated values were obtained using equation (13), the case of a semi-infinite exponentially converging aquifer. The per-cent relative deviation between the values ranged from 0.07% to 23.14%.

Figures 4 and 5 represent steady-state head distributions of representative samples of the data collected. Figure 4 is a plot of three steady-state profiles for a diverging aquifer. The solid lines are the theoretical curves computed from equation (10). A small sketch

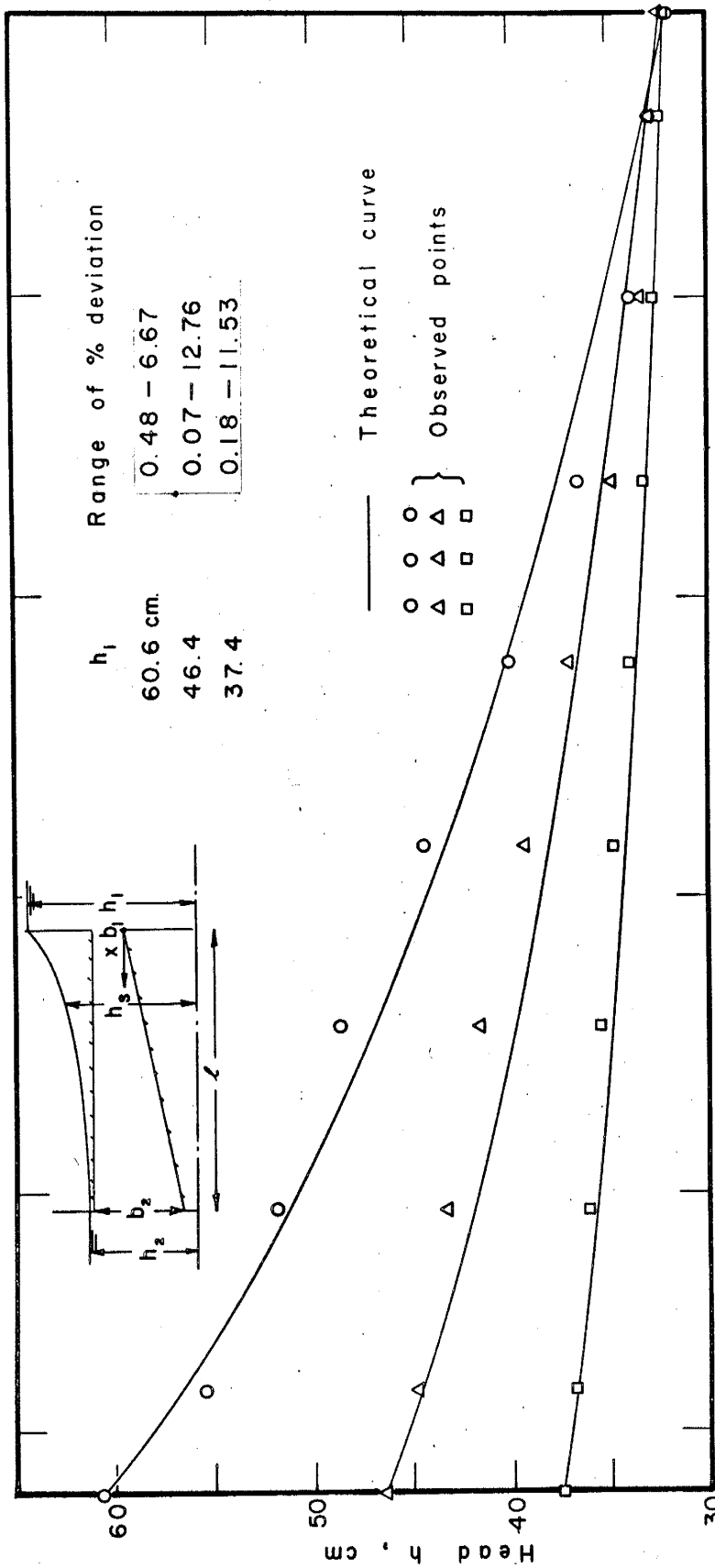

Fig.4 Steady-state head distribution in a wedge-shaped aquifer connecting two parallel reservoirs

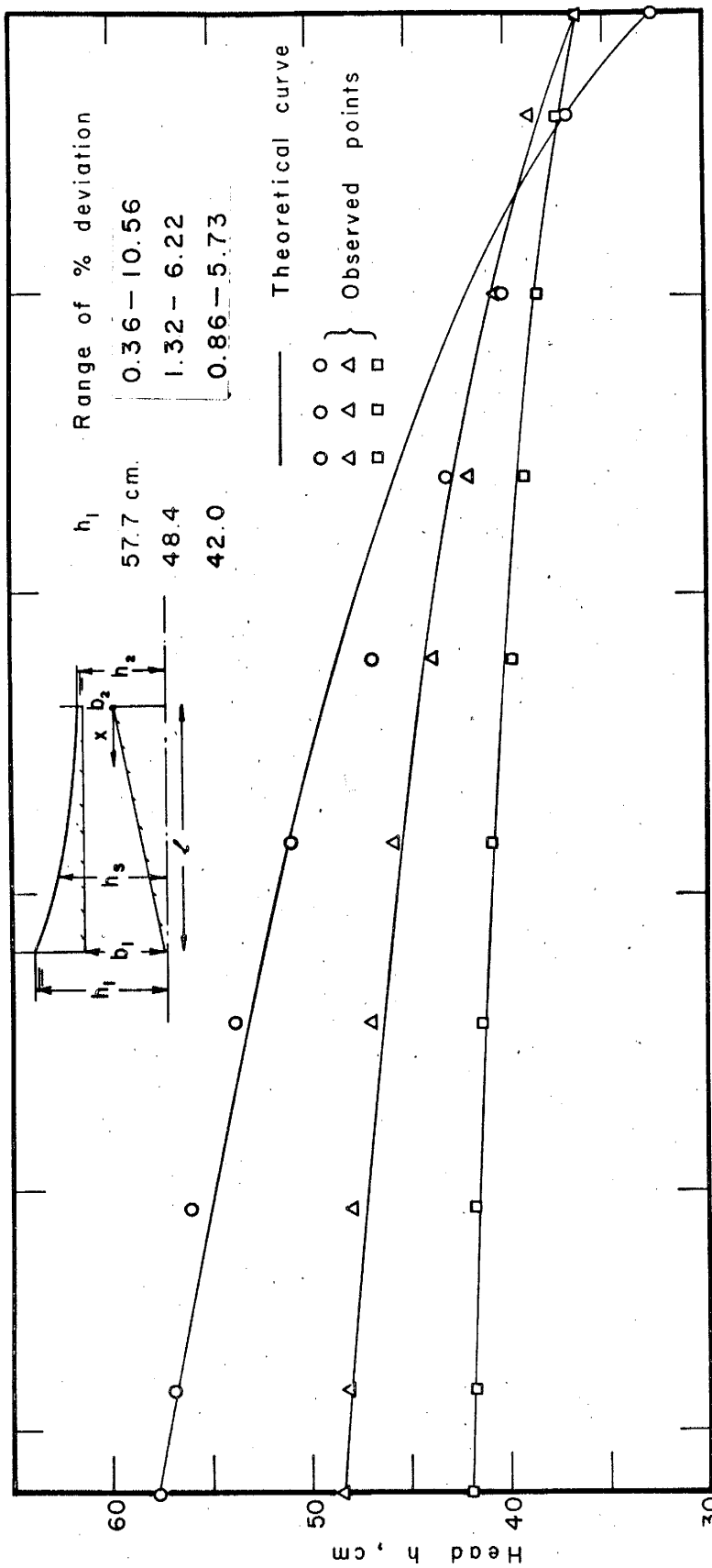

Fig.5 Steady-state head distribution in a wedge-shaped aquifer connecting two parallel reservoirs

of the flow system is inserted in each drawing for clarity of interpretation. The range of per-cent deviation for each run is also presented.

Figure 5 is a steady-state graph for a converging aquifer between two streams. The theoretical curves were computed using a 180° rotation of equation (10). The similarity in the profiles of figures 4 and 5 is apparent if a 180° rotation is effected. In both figures 4 and 5 the average hydraulic head in cm is plotted against distance, x or ℓ - x, in cm.

The trend of the deviations in the steady-state cases is quite different from that of the unsteady-state cases. For example, a curve drawn through the observed points in figure 4 would have the main inflection point at approximately 140 cm. The minimum deviations occur at or near this point while maximum deviations occur at about 40 cm on either side. These maximum deviations are roughly of the same order of magnitude, which suggests that the modeling error is evenly distributed. Since, in the steady state, the plate spacing does not enter into the equations for head, it is suggested that this definite pattern of error is built into the model in some other fashion. Possibly, the diameter of the storage tubes is not correct, or the spacing of the tubes is the dominant factor. On the other hand, it is possible that the Hele-Shaw model just is not capable of a much greater accuracy.

Figures 6, 7, and 8 are plots of the average hydraulic heads versus distance for different times, after the head had been increased instantaneously. Three different representative sudden changes in head in a semi-infinite linearly diverging aquifer have been shown. The the-

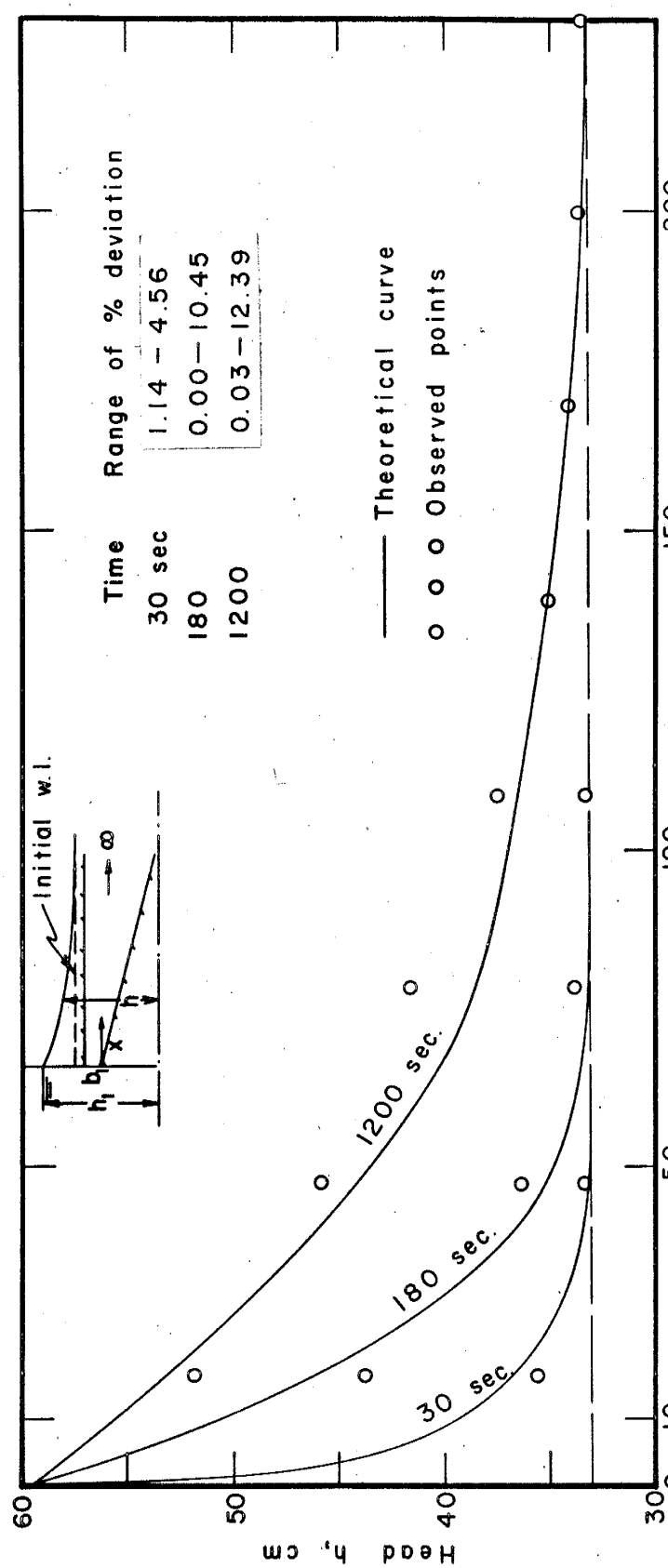

Fig. 6 Variation of head with time in a semi-infinite wedge-shaped aquifer for $h_1 = 59.6$ cm, $h_i = 33.3$ cm

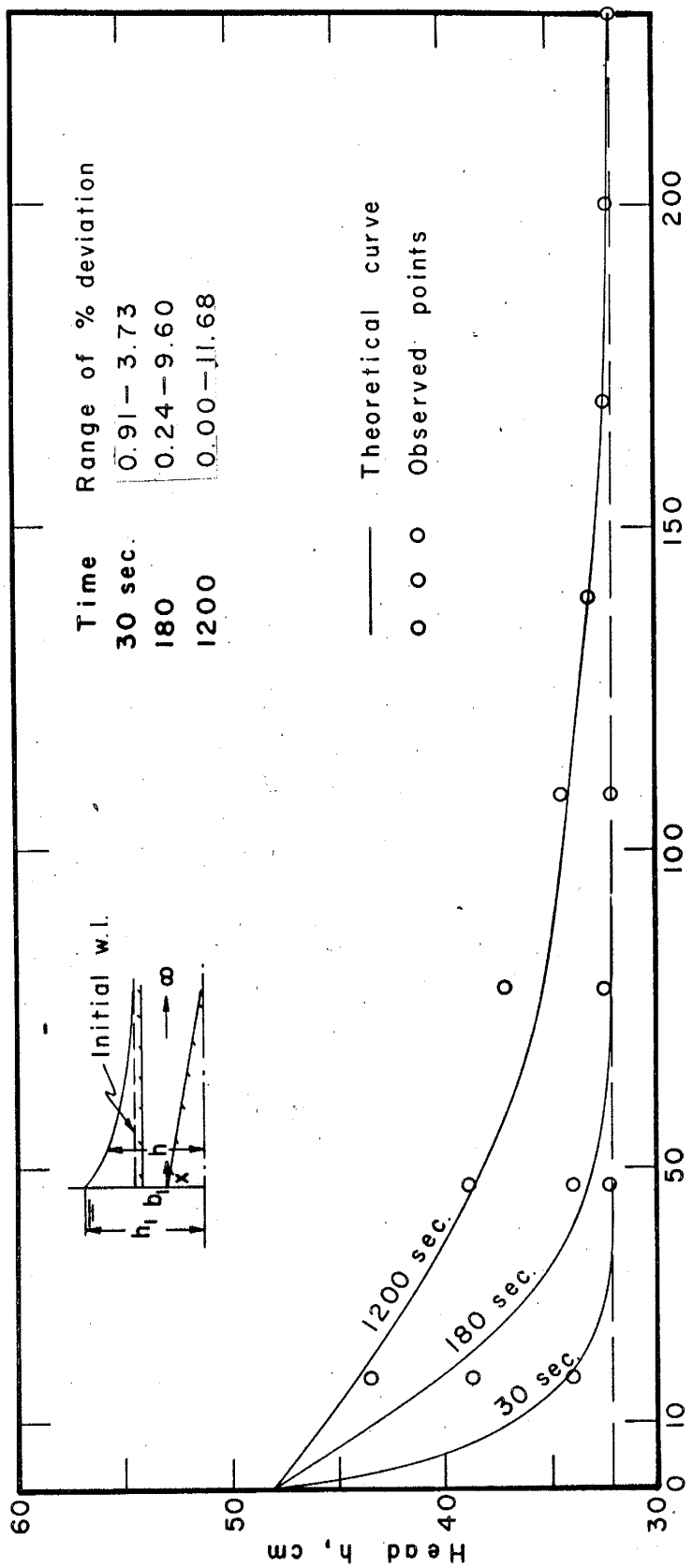

Fig. 7 Variation of head with time in a semi-infinite wedge-shaped aquifer for $h_1 = 48.4$ cm, $h_i = 32.0$ cm

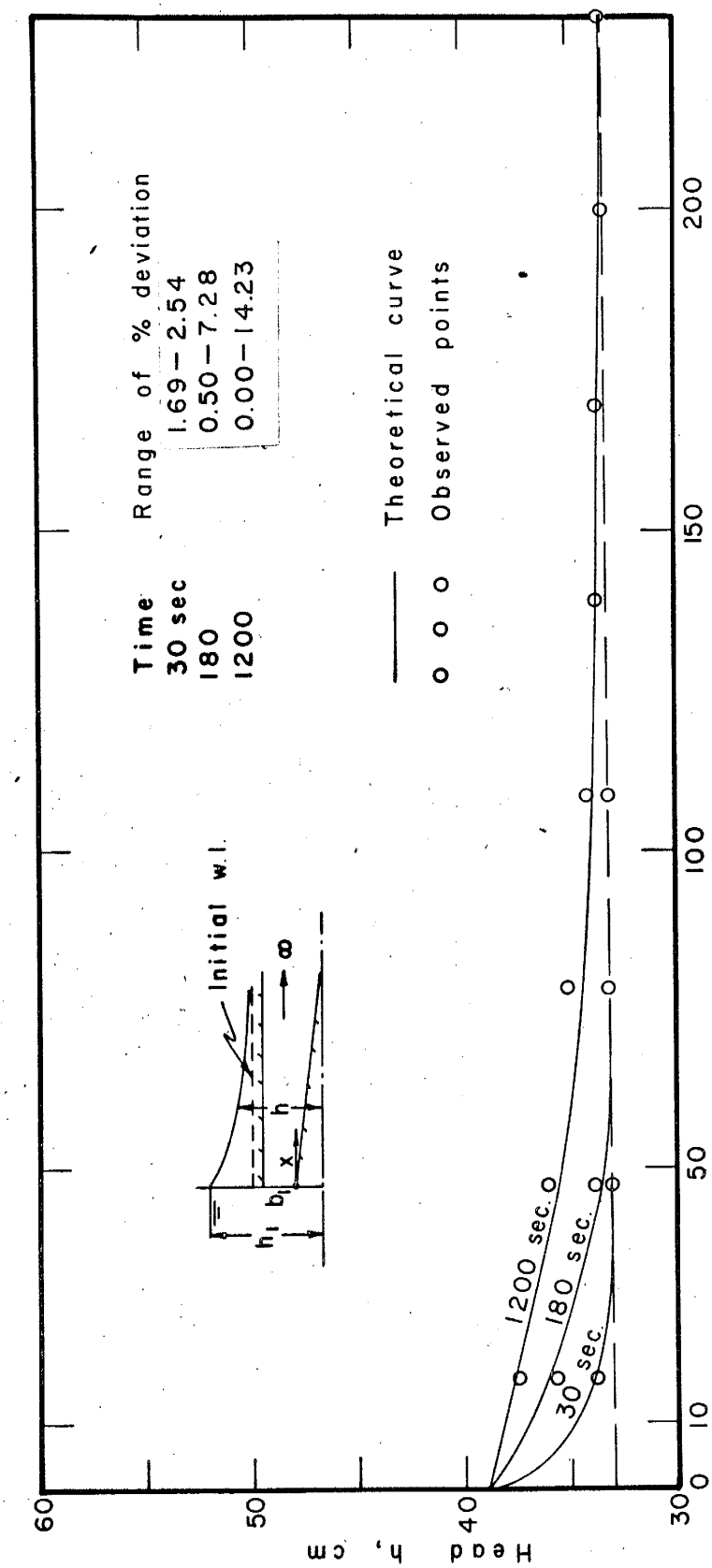

Fig.8 Variation of head with time in a semi-infinite wedge-shaped aquifer for $h_1 = 39.0$ cm, $h_i = 33.1$ cm

oretical curves were computed using equation (8).

In figures 6, 7, and 8 there is again a definite trend in the deviation of the observed points from the theoretical curve, different from both the steady-state trend and from the trend noticed in figures 9, 10, and 11. The main inflection point in a curve traced through each of the sets of observed points would fall around 75 cm from the source of flow. This pattern is independent of time, which suggests that a modeling error of some kind exists. The maximum deviation occurs at or near this inflection point, with the error decreasing on either side, and being much less the farther away from the source of flow one goes. This error is possibly due to the incorrect modeling of the aquifer's storage and is showing up in a definite pattern. Another contributing factor could be the variation in plate spacing at this point in the aquifer. But, as in the steady-state cases, these deviations are only of about second-order magnitude and less.

Figures 9, 10, and 11 show hydraulic-head profiles at different times for a sudden change in head effected in a semi-infinite linearly converging wedge-shaped aquifer. In these graphs the theoretical curves were computed using equation (13). In this flow system the mathematical model was an exponentially thinning-out aquifer assumed to extend to infinity.

In figures 9, 10, and 11 the maximum deviations occur at or near 50 cm from the source of flow. This is the main inflection point for the curves passed through the observed points. The trend is again independent of time and reservoir head, but in contrast to

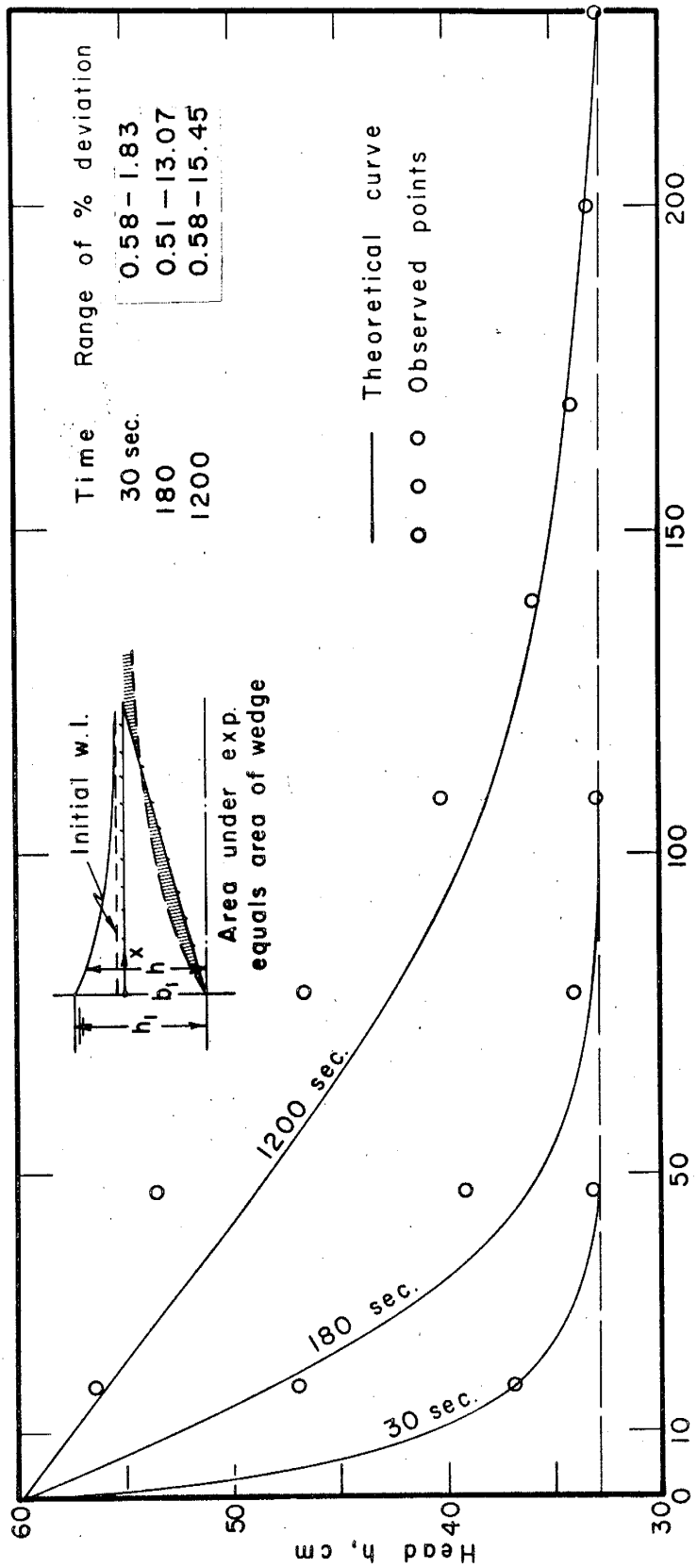

Fig.9 Variation of head with time in a pinching out aquifer for $h_1 = 60.0$ cm , $h_i = 32.7$ cm

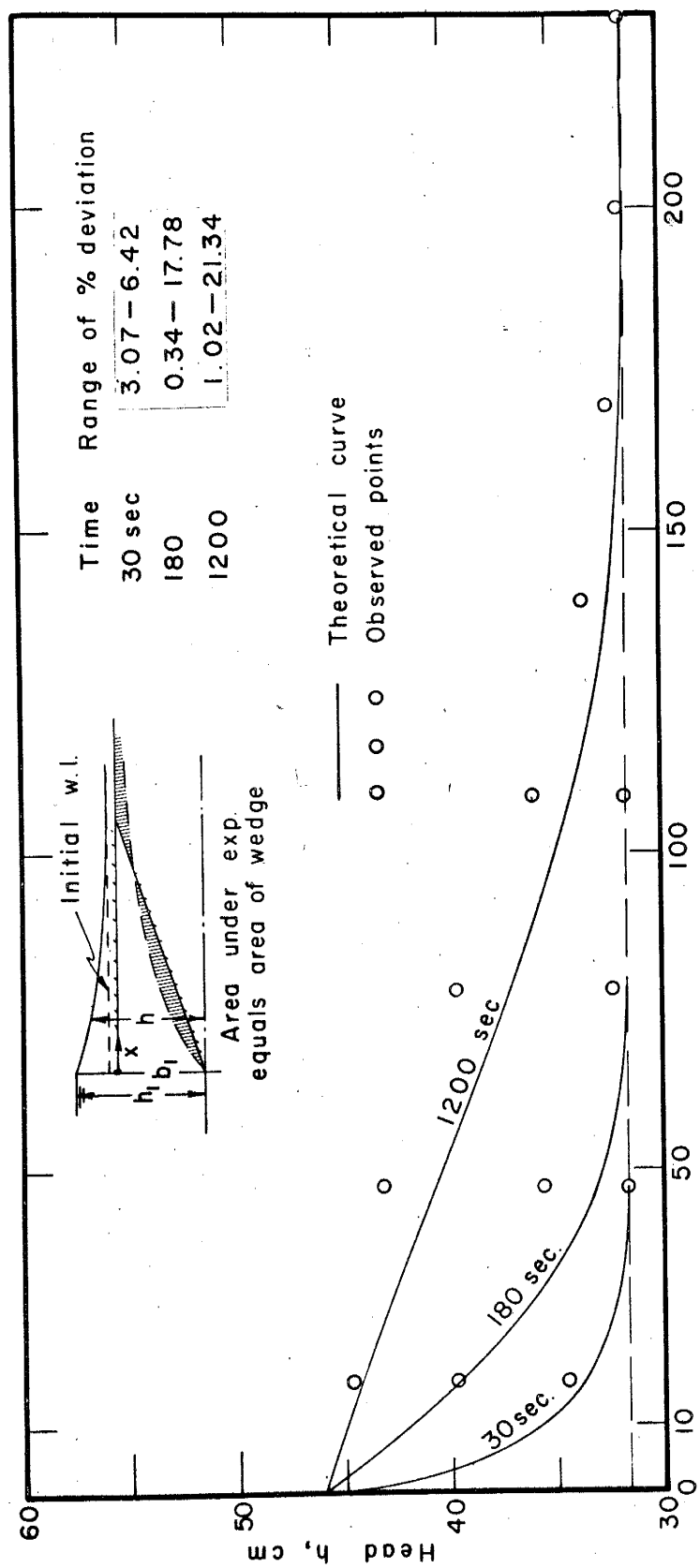

Fig.10 Variation of head with time in a pinching out aquifer for $h_1 = 46.0$ cm , $h_i = 31.5$ cm

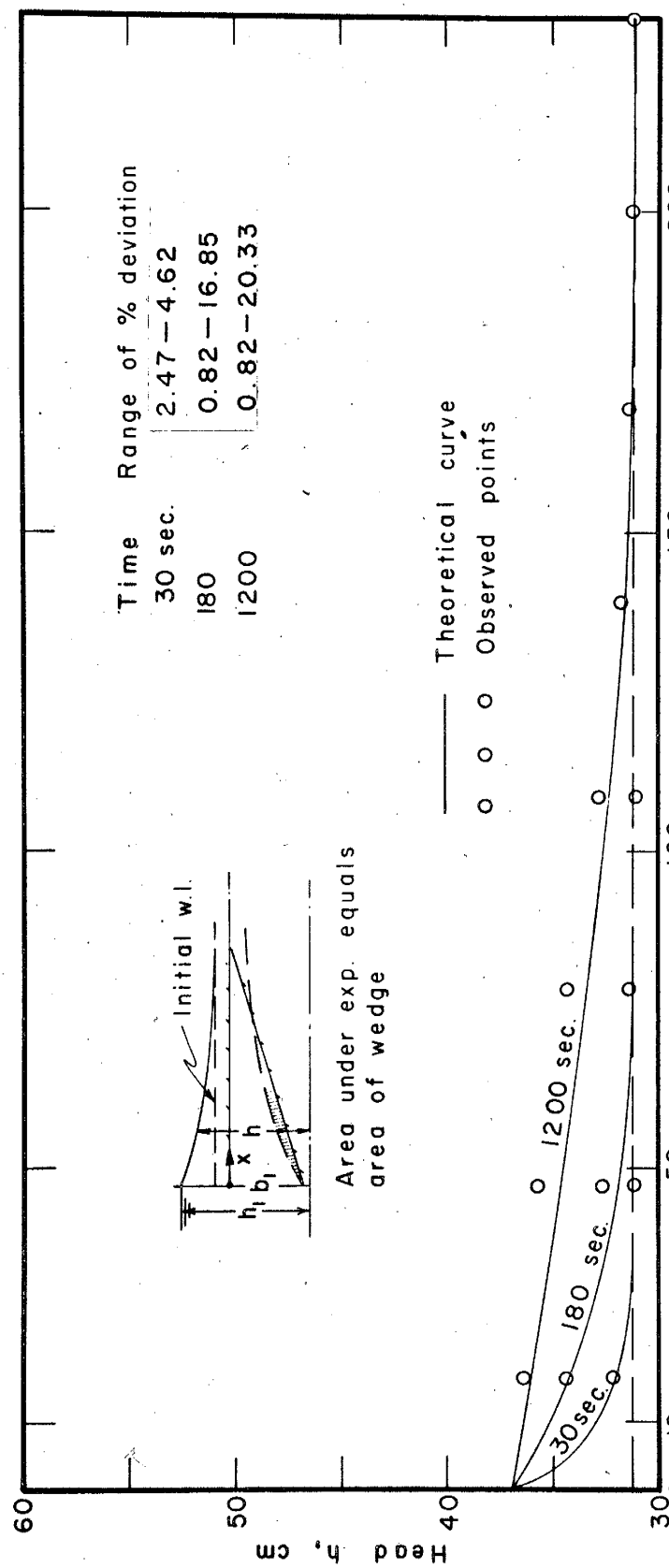

Fig.11 Variation of head with time in a pinching out aquifer for $h_1 = 37.0$ cm , $h_i = 31.0$ cm

figures 6, 7, and 8 the deviations fall in a somewhat different pattern. For one thing, the maximum deviations are on the average greater, and these maximum deviations occur closer to the source of flow. The deviations in the first tube in these figures are relatively small as compared to the deviations of the first tube in the last set of figures. These deviations in figures 9, 10, and 11 could be due to the same reasons mentioned about figures 6, 7, and 8. On the other hand, the deviations could possibly be explained by the matching of the type of theoretical curve applied; that is to say, the approximation of the exponentially thinning-out aquifer may, and undoubtedly is, contributing to the deviations.

In all of the cases considered in this discussion, one must realize that the present model-prototype analogy is not in the practical range. For example, most wedge-shaped aquifers are several thousands of feet in length. A practical sudden change in head in a stream, or ditch, is of the order of 10 feet. This practical change in head of 10 feet would scale down in the present model to a few millimeters.

The theory asserts that the flow in wedge-shaped aquifers cannot be approximated by that which would exist in aquifers of uniform thickness, except during very short-time periods which become longer as one approaches the source of flow. The experimental results confirm this conclusion. Figures 12 and 13 are comparisons of the solution for a wedge-shaped sand in the direction of divergence and a sand of uniform thickness, respectively. Figure 12 is the comparison in the steady-state, and Figure 13 in the unsteady-state. The approximation under discussion is strictly limited to the unsteady case, and

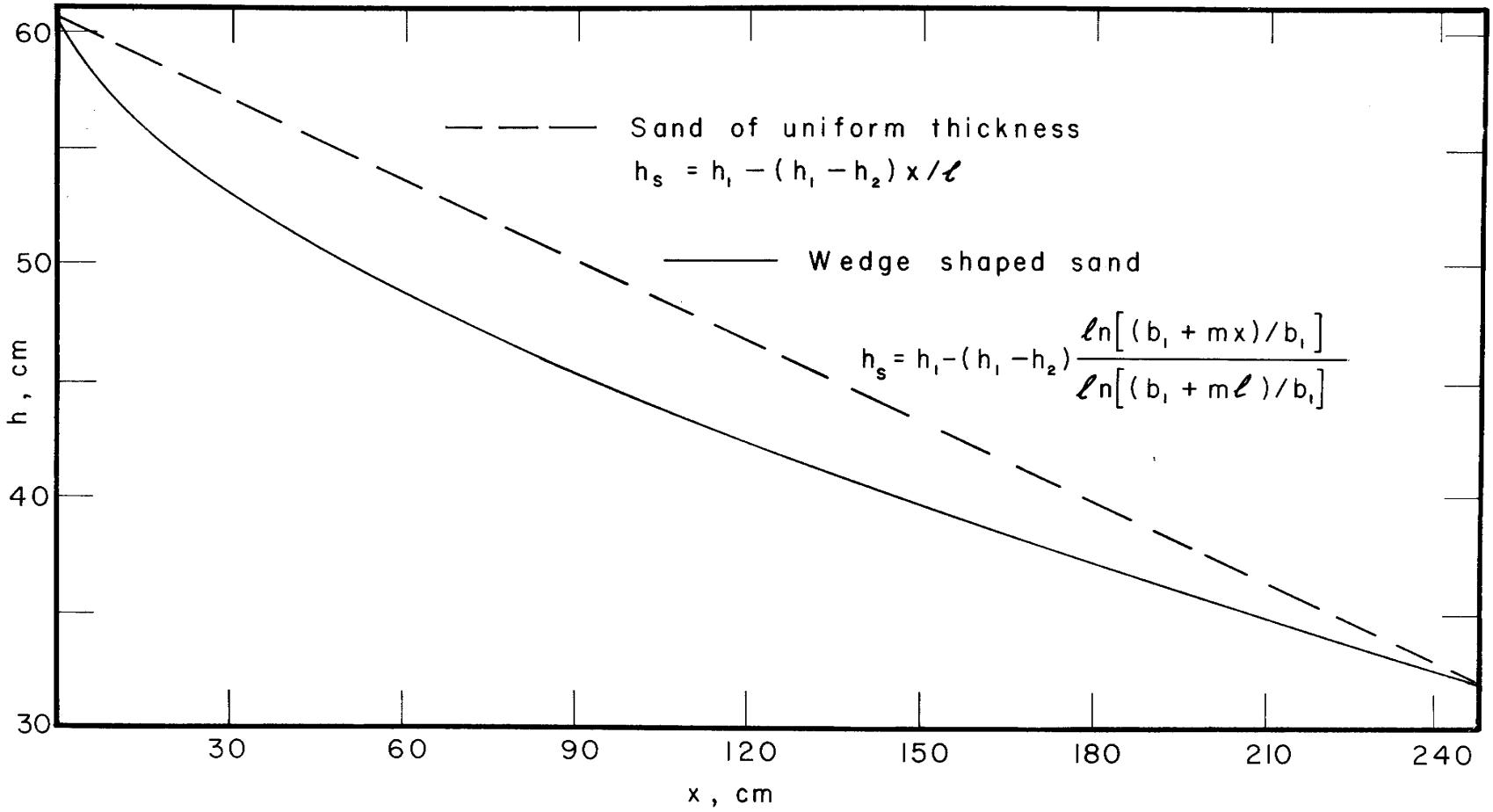

Fig.12 Comparison graph of steady-state head distribution in model for h_1 = 60.6 cm

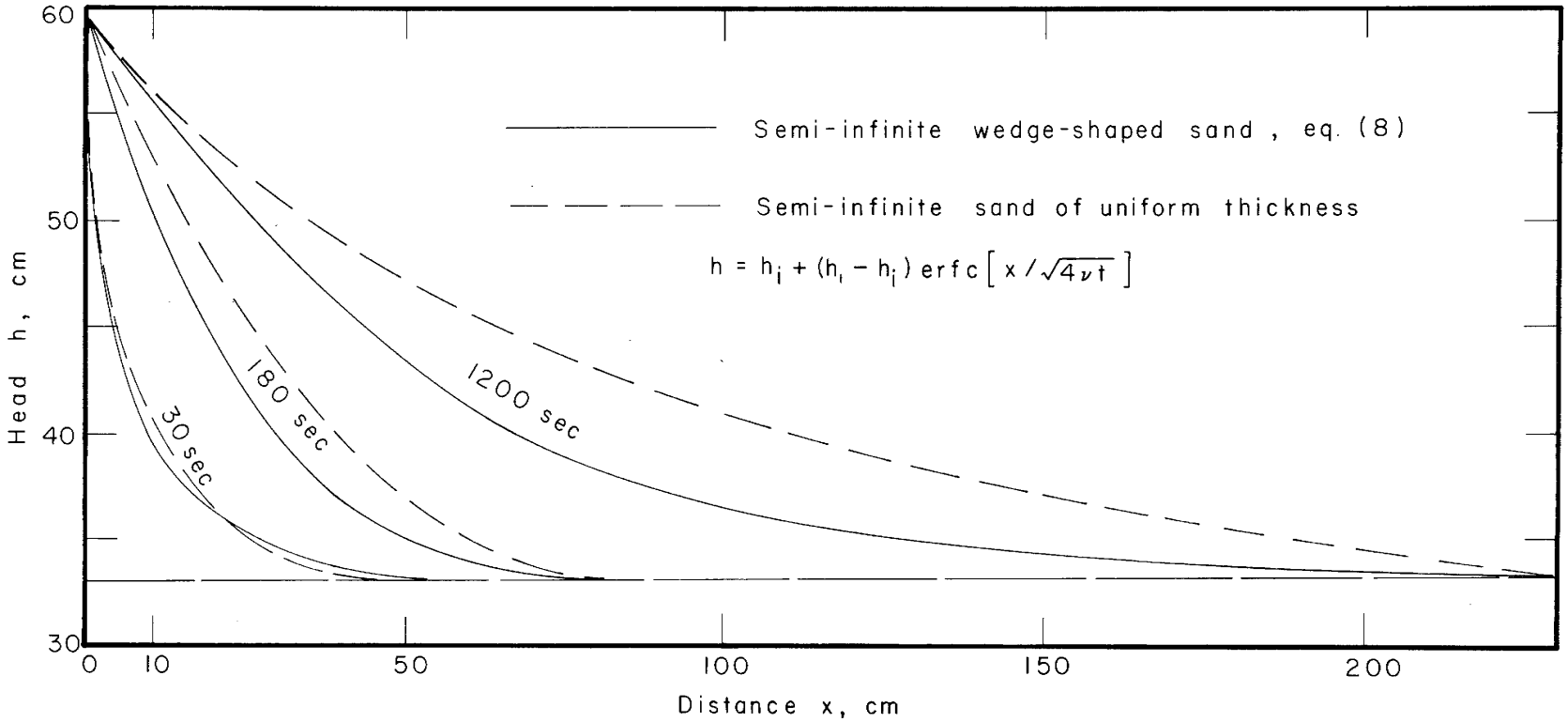

Fig. 13 Comparison graph for unsteady-state head distribution between a semi-infinite linearly diverging aquifer and an aquifer of uniform thickness for $h_1 = 59.6$ cm , $h_i = 33.3$ cm

even here it is applicable only for very short time periods near the source of flow.

It is clear that the experimental results, in general, show good agreement with the analytical expressions for the cases tested.

CONCLUSIONS

The present investigation leads to the following conclusions:

1) The experimental results are in agreement with those obtained analytically, within the ranges tested, thus establishing the validity of equations (8), (10), and (13) and of their approximations.

2) The assumption that the vertical component of velocity be neglected appears justified by the experimental results.

3) A semi-infinite linearly converging wedge-shaped aquifer can be approximated by an exponentially decreasing system provided the slopes are kept at less than 0.20.

4) The flow in wedge-shaped aquifers cannot be approximated by that which would exist if the aquifer were of uniform thickness except during very short periods of time which become longer as the source of flow is approached.

RECOMMENDATIONS FOR FUTURE WORK

In modeling an artesian aquifer, the biggest problem is to simulate the storage. This, as previously stated, appears to be the greatest factor contributing to the deviations. In a future model of this type I would suggest a spacing of the storage tubes on the order of 10 or 12 cm. Also, I would reduce the slots connecting the back plate and the storage tubes from a width of 0.635 cm to 0.250 cm, and make them exactly equal to the depth of the aquifer. In my estimation, these modifications would model the specific storage more accurately and cut down the circulation in the storage tubes. I would space the piezometer tubes, if at all needed, directly opposite the storage tubes in the front plate. In this fashion one could observe the average head as well as the exact head at different points in the aquifer.

A greater density of spacing washers would maintain the geometry of the model without materially influencing the flow.

A system of sliding gates between the reservoirs and the aquifer is desirable, so that a sudden change of head can be obtained instantaneously. In conjunction with these gates, a large hose or hoses, connecting the Mariotte bottle to the reservoir, is also needed. This is due to the high viscosity of the oil as compared to water. These large hoses would provide more continuity between the constant-head supply reservoir and the model reservoir. I recommend these hoses to be of at least one inch inside diameter.

APPENDIX I

TABLE I: Steady-State Data (Diverging Case)

x cm	h_o	h_c	% dev	h_o	h_c	% dev
0.00	60.60	60.60		46.35	46.35	
17.14	55.45	56.66	4.23	44.85	44.84	0.07
47.62	51.90	51.30	2.09	43.30	42.02	9.07
78.10	48.70	46.79	6.67	41.60	39.80	12.76
108.58	44.40	43.22	4.12	39.38	38.04	9.50
139.06	40.00	40.14	0.48	36.97	36.41	3.97
169.54	36.50	37.51	3.53	34.85	35.06	1.48
200.02	33.85	35.20	4.72	33.35	33.88	4.11
230.50	32.80	33.09	1.01	32.75	32.81	0.42
247.65	32.00	32.00		32.25	32.25	
	h_1 = 60.60 cm h_2 = 32.00 cm ℓ = 247.65 cm h_c computed from Eq. (10)			h_1 = 46.35 cm h_2 = 32.25 cm ℓ = 247.65 cm h_c computed from Eq. (10)		

TABLE I: (cont'd) Steady-State Data (Diverging Case)

x cm	h_o	h_c	% dev
0.00	37.45	37.45	
17.14	36.70	36.72	0.37
47.62	36.05	35.70	6.61
78.10	35.50	34.89	11.53
108.58	34.80	34.24	10.58
139.06	33.95	33.68	5.10
169.54	33.23	33.19	0.75
200.02	32.62	32.75	2.45
230.50	32.35	32.36	0.18
247.65	32.16	32.16	

h_1 = 37.45 cm

h_2 = 32.16 cm

ℓ = 247.65 cm

h_c computed from Eq. (10)

TABLE II: Steady-State Data (Converging Case)

x cm	h_o	h_c	% dev	h_o	h_c	% dev
0.00	57.70	57.70		48.45	48.45	
17.14	56.90	56.81	0.36	48.20	48.04	1.32
47.62	56.10	55.16	3.76	47.90	47.24	5.47
78.10	53.80	53.30	2.00	46.90	46.34	2.98
108.58	50.80	51.16	1.44	45.60	45.32	2.32
139.06	46.80	48.68	7.52	43.70	44.11	3.40
169.54	43.00	45.64	10.56	41.90	42.65	6.22
200.02	40.00	41.82	7.28	40.40	40.81	3.40
230.50	36.80	36.68	0.56	38.70	38.33	3.07
247.65	32.72	32.72		36.40	36.40	
	h_1 = 57.70 cm h_2 = 32.72 cm ℓ = 247.65 cm h_c computed from a 180° rotation of Eq. (10)			h_1 = 48.45 cm h_2 = 36.40 cm ℓ = 247.65 cm h_c computed from a 180° rotation of Eq. (10)		

TABLE II: (cont'd) Steady-State Data (Converging Case)

x cm	h_o	h_c	% dev
0.00	42.05	42.05	
17.14	41.90	41.85	0.86
47.62	41.80	41.47	5.73
78.10	41.30	41.04	4.52
108.58	40.70	40.56	2.43
139.06	39.80	39.98	3.13
169.54	39.00	39.28	4.86
200.02	38.30	38.40	1.73
230.50	37.40	37.22	3.13
247.65	36.30	36.30	

h_1 = 42.05 cm

h_2 = 36.30 cm

ℓ = 247.65 cm

h_c computed from a 180° rotation of Eq. (10)

TABLE III: Unsteady-State Data (Semi-infinite Case)

x cm	h_i = 33.00	33.00	33.10	33.15	33.30	33.30	33.40	33.45	33.45
t sec	0.00	17.14	47.62	78.10	108.58	139.06	169.54	200.02	230.50
30	h_o	35.50	33.40						
	% dev	4.56	1.14						
	h_c	36.70	33.10						
60	h_o	38.10	33.90	33.25					
	% dev	8.97	2.73	0.38					
	h_c	40.46	33.18	33.15					
90	h_o	40.00	34.50	33.30					
	% dev	10.91	3.87	0.57					
	h_c	42.87	33.48	33.15					
120	h_o	41.50	35.20	33.50					
	% dev	10.95	4.86	1.29					
	h_c	44.38	33.92	33.16					
180	h_o	43.70	36.40	33.90	33.40	33.32			
	% dev	10.45	5.24	2.47	0.15	0.00			
	h_c	46.45	35.02	33.25	33.36	33.32			
300	h_o	46.40	38.60	35.00	33.65	33.38			
	% dev	8.47	5.85	4.86	0.03	0.22			
	h_c	48.63	37.06	33.72	33.66	33.44			
600	h_o	49.50	42.25	37.80	34.80	33.70	33.50	33.50	
	% dev	5.93	6.31	8.74	0.03	0.91	0.26	0.11	
	h_c	51.06	40.59	35.50	34.81	33.94	33.43	33.47	
1200	h_o	51.90	45.95	41.70	37.55	35.00	34.00	33.65	33.55
	% dev	3.84	7.30	12.39	2.69	0.03	0.76	0.11	0.19
	h_c	52.91	44.03	38.44	36.84	35.01	33.80	33.68	33.50

h_i = initial head

h_o = observed head

h_c = calculated head from Eq. (8)

h_1 = 59.60 cm

TABLE III: (cont'd) Unsteady-State Data (Semi-infinite Case)

x cm	h_i = 32.15	32.05		32.05		32.00		32.00		31.95		31.95		31.92		31.93	
t sec	0.00	17.14		47.62		78.10		108.58		139.06		169.54		200.02		230.50	
30	h_o	33.70	3.73	32.20	0.91												
	% dev																
	h_c	34.31		32.05													
60	h_o	35.30	5.56	32.50	2.44												
	% dev																
	h_c	36.61		32.10													
90	h_o	36.30	10.88	32.80	3.18	32.10	0.61										
	% dev																
	h_c	38.08		32.28		32.00											
120	h_o	37.40	9.78	33.20	3.97	32.20	1.22	32.05	0.30								
	% dev																
	h_c	39.00		32.55		32.00		32.00									
180	h_o	38.70	9.60	34.00	4.77	32.40	2.20	32.10	0.36	32.00	0.24						
	% dev																
	h_c	40.27		33.22		32.06		32.04		31.96							
300	h_o	40.40	7.33	35.30	5.07	33.10	4.58	32.20	0.12	32.00	0.24						
	% dev																
	h_c	41.60		34.47		32.35		32.22		32.04							
600	h_o	42.15	5.74	37.60	5.93	34.75	8.01	32.85	0.42	32.20	0.85	31.99	0.12	31.99	0.36		
	% dev																
	h_c	43.09		36.63		33.44		32.92		32.34		31.97		31.93			
1200	h_o	43.50	4.40	39.85	6.85	37.15	11.68	34.55	2.38	33.00	0.00	32.30	0.61	32.05	0.06	31.95	0.06
	% dev																
	h_c	44.22		38.73		35.24		34.16		33.00		32.20		32.06		31.96	

h_i = initial head

h_o = observed head

h_c = calculated head from Eq. (8)

h_1 = 48.35 cm

TABLE III (cont'd) Unsteady-State Data (Semi-infinite Case)

x cm	h_i = 32.95	33.00	33.00	33.05	33.10	33.22	33.30	33.30	33.30
t sec	0.00	17.14	47.62	78.10	108.58	139.06	169.54	200.02	230.50
30	h_o	33.70	33.10						
	% dev	2.54	1.69						
	h_c	33.85	33.00						
60	h_o	34.30	33.20	33.10					
	% dev	6.94	3.05	0.84					
	h_c	34.71	33.02	33.05					
90	h_o	34.75	33.35	33.10					
	% dev	8.64	4.06	0.84					
	h_c	35.26	33.09	33.05					
120	h_o	35.10	33.50	33.15	33.15				
	% dev	8.64	5.25	1.69	0.84				
	h_c	35.61	33.19	33.05	33.10				
180	h_o	35.65	33.80	33.20	33.15	33.25			
	% dev	7.28	6.10	2.20	0.67	0.50			
	h_c	36.08	33.44	33.07	33.11	33.22			
300	h_o	36.20	34.30	33.50	33.20	33.25			
	% dev	6.44	6.61	5.42	0.33	0.00			
	h_c	36.58	33.91	33.18	33.18	33.25			
600	h_o	37.00	35.20	34.20	33.50	33.40	33.30		
	% dev	2.37	8.13	10.33	1.01	0.67	0.16		
	h_c	37.14	34.72	33.59	33.44	33.36	33.31		
1200	h_o	37.40	36.10	35.10	34.20	33.70	33.40	33.31	33.31
	% dev	2.71	10.00	14.23	4.91	1.52	0.16	0.67	0.00
	h_c	37.56	35.51	34.26	33.91	33.61	33.39	33.35	33.31

h_i = initial head

h_o = observed head

h_c = calculated head from Eq. (8)

h_1 = 39.00 cm

TABLE IV Unsteady-State Data (Pinching-out Case)

x cm	h_i = 32.80	32.80	32.80	32.80	32.75	32.65	32.60	32.60	32.60
t sec	0.00	17.14	47.62	78.10	108.58	139.06	169.54	200.02	230.50
30	h_o	36.80	33.30						
	% dev	0.58	1.83						
	h_c	36.64	32.80						
60	h_o	40.00	34.30	32.90					
	% dev	4.68	5.09	0.36					
	h_c	41.28	32.91	32.80					
90	h_o	42.40	35.40	33.10	32.80				
	% dev	6.15	7.47	1.09	0.18				
	h_c	44.08	33.36	32.80	32.75				
120	h_o	44.20	36.80	33.20	32.80				
	% dev	6.63	10.03	1.35	0.18				
	h_c	46.01	34.06	32.83	32.75				
180	h_o	47.00	39.30	34.00	32.90				
	% dev	5.42	13.07	3.62	0.51				
	h_c	48.48	35.73	33.01	32.76				
300	h_o	50.40	43.30	35.70	33.30	32.75	32.62		
	% dev	2.78	16.04	6.37	1.57	0.32	0.07		
	h_c	51.16	38.92	33.96	32.87	32.66	32.60		
600	h_o	54.10	49.20	40.60	35.40	33.35	32.80	32.65	
	% dev	0.18	18.68	11.79	4.98	1.42	0.54	0.14	
	h_c	54.05	44.10	37.38	34.14	32.96	32.65	32.61	
1200	h_o	56.50	53.70	46.70	40.30	35.70	33.95	33.25	32.85
	% dev	1.97	17.14	15.45	8.31	2.23	1.42	1.17	0.58
	h_c	55.96	49.02	42.48	38.03	35.09	33.56	32.93	32.69

h_i = initial head

h_o = observed head

h_c = calculated head from Eq. (13)

h_1 = 60.00 cm

TABLE IV: (cont'd) Unsteady-State Data (Pinching-out Case)

x cm	h_i = 31.60	31.45	31.45	31.40	31.38	31.38	31.38	31.34	31.30
t sec	0.00	17.14	47.62	78.10	108.58	139.06	169.54	200.02	230.50
30	h_o	34.50	31.90						
	% dev	6.42	3.07						
	h_c	33.56	31.45						
60	h_o	36.10	32.60						
	% dev	1.09	7.45						
	h_c	35.94	31.51						
90	h_o	37.30	33.30	31.60					
	% dev	0.82	10.67	1.36					
	h_c	37.42	31.74	31.40					
120	h_o	38.40	34.10	31.75	31.40				
	% dev	0.27	13.54	2.32	0.13				
	h_c	38.44	32.12	31.41	31.38				
180	h_o	39.70	35.60	32.30	31.50				
	% dev	0.34	17.78	5.40	0.82				
	h_c	39.75	33.00	31.51	31.38				
300	h_o	41.40	37.80	33.50	31.80	31.45			
	% dev	1.57	21.27	10.19	2.46	0.47			
	h_c	41.17	34.69	32.01	31.44	31.38			
600	h_o	43.40	40.80	36.50	33.15	31.87	31.50	31.38	
	% dev	4.78	23.05	18.33	7.04	2.12	0.61	0.27	
	h_c	42.70	37.43	33.82	32.12	31.54	31.41	31.34	
1200	h_o	44.60	43.10	39.65	35.90	33.50	32.25	31.75	31.50
	% dev	6.08	20.93	21.34	11.76	5.67	2.46	1.64	1.02
	h_c	43.71	40.04	36.53	34.18	32.67	31.89	31.51	31.35

h_i = initial head

h_o = observed head

h_c = calculated head from Eq. (13)

h_1 = 46.00 cm

TABLE IV: (cont'd) Unsteady-State Data (Pinching-out Case)

x cm	h_i = 31.10	31.05	31.05	31.05	30.95	30.89	30.85	30.82	30.73
t sec	0.00	17.14	47.62	78.10	108.58	139.06	169.54	200.02	230.50
30	h_o	32.20	31.20						
	% dev	4.62	2.47						
	h_c	31.92	31.05						
60	h_o	32.95	31.50	31.10					
	% dev	0.99	7.10	0.82					
	h_c	32.89	31.07	31.05					
90	h_o	33.50	31.80	31.12					
	% dev	0.00	10.41	1.15					
	h_c	33.50	31.17	31.05					
120	h_o	33.89	32.10	31.20	30.98				
	% dev	0.49	12.89	2.31	0.49				
	h_c	33.92	31.32	31.06	30.95				
180	h_o	34.40	32.70	31.30	31.00				
	% dev	0.82	16.85	3.30	0.82				
	h_c	34.45	31.68	31.10	30.95				
300	h_o	35.10	33.60	31.80	31.10	30.90			
	% dev	1.15	20.16	8.26	1.98	0.16			
	h_c	35.03	32.38	31.30	30.98	30.89			
600	h_o	35.90	34.90	33.00	31.70	31.10	30.90	30.85	
	% dev	3.96	23.14	15.86	7.43	2.31	0.82	0.49	
	h_c	35.66	33.50	32.04	31.25	30.96	30.85	30.82	
1200	h_o	36.40	35.80	34.28	32.82	31.73	31.25	31.00	30.80
	% dev	5.45	20.33	18.67	11.90	5.12	3.14	1.81	0.82
	h_c	36.07	34.57	33.15	32.10	31.42	31.06	30.89	30.75

h_i = initial head

h_o = observed head

h_c = calculated head from Eq. (13)

h_1 = 37.00 cm

TABLE V Effective storage tube area, and diameters of the compensating rods as determined from:

$$\text{Specific Storage of the Model} = \frac{(\text{cross sectional area of storage tube})(\text{unit head decline})}{(\text{volume of aquifer segment})(\text{unit head decline})}$$

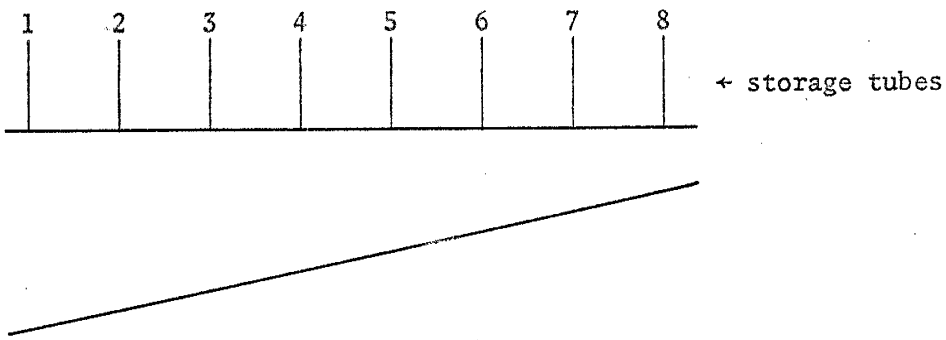

	1	2	3	4	5	6	7	8
Effective storage tube area in inches^2	0.785	0.706	0.633	0.560	0.479	0.399	0.323	0.236
Diameter of compensating rods in inches	0.000	0.317	0.441	0.536	0.624	0.702	0.767	0.837

APPENDIX II

The oil used in this investigation is marketed as Shell Tellus Oil 72. A chart of kinematic viscosity in centistokes versus temperature in degrees Fahrenheit is presented in figure 14. The values shown in this figure were interpolated from observed data, using Chart E of ASTM Standard Viscosity-Temperature Charts for Liquid Petroleum Products (D-341). Both the oil and the chart were kindly supplied by the Wilmington (California) Refinery of Shell Oil Company, courtesy of Mr. L. A. Shaw.

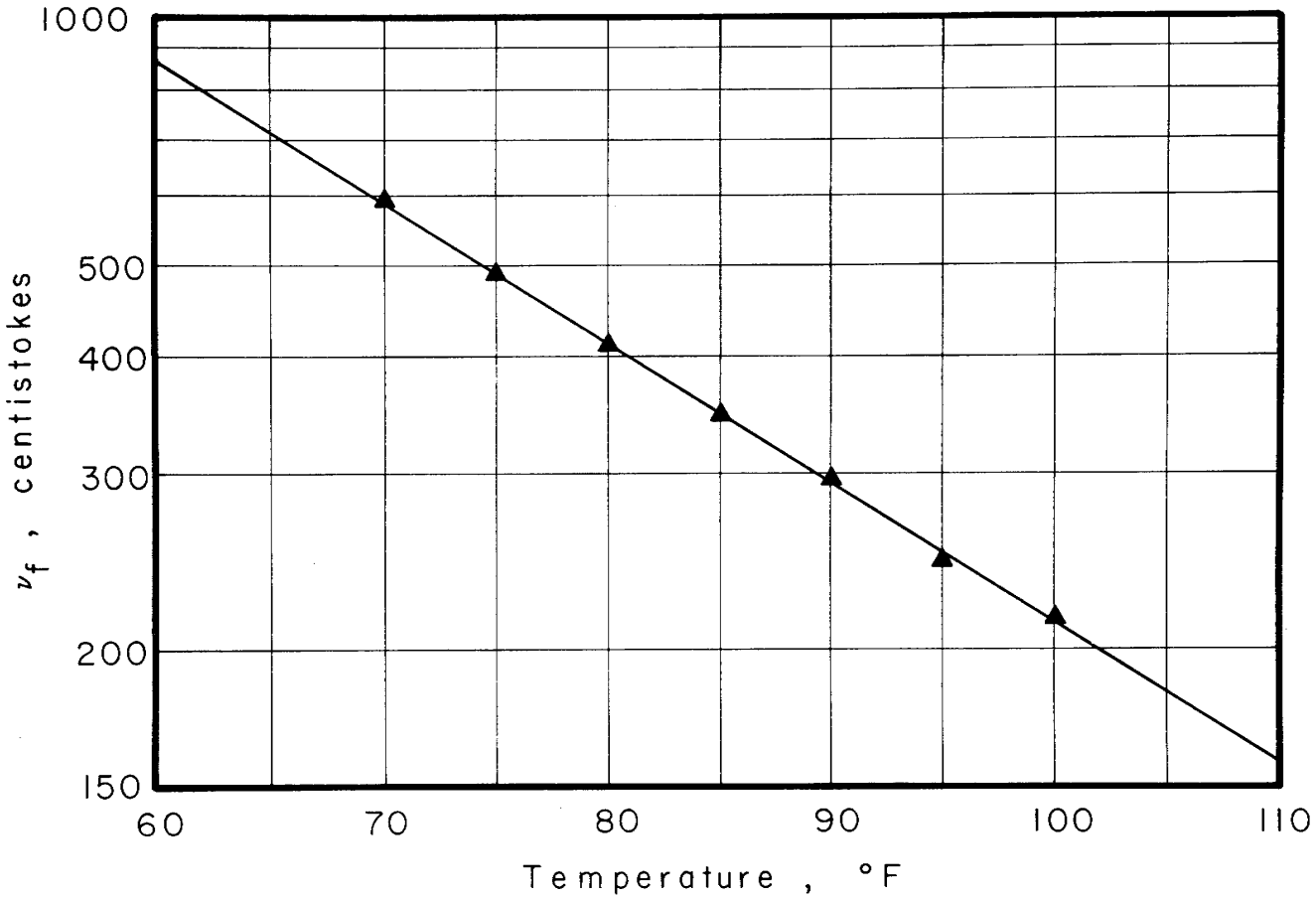

Fig. 14 Relationship between kinematic viscosity and temp. for Shell's *Tellus* oil # 72.

APPENDIX III

The following is a list of the major symbols and definitions used in the text:

$A(x,t)$	:	the flowing well function (an infinite integral);
a	:	a geometrical parameter defining the exponential variation of the aquifer's thickness;
b, b_1, b_2	:	the aquifer thickness at any distance x, at reservoir 1, and at reservoir 2 respectively;
$\text{erfc}(x)$	:	the complementary error function;
$f_1(x,y)$, $f_2(x,y)$	:	function of x and y defining the surfaces which confine the water-bearing material;
$h(x,y,t)$	:	the average piezometric head in a vertical column of the aquifer located at the point (x,y) referred to an arbitrary datum of elevation;
h_1, h_2	:	constant water levels at specified boundaries of the aquifer (reservoirs 1 and 2);
h_i	:	initial head in a flow system;
h_s	:	the average head during steady-state flow;
K	:	the hydraulic conductivity of the aquifer;
ℓ	:	horizontal distance between two parallel boundaries of a flow system;
m_1, m_2	:	the slopes of the upper and lower confining beds of a wedge-shaped aquifer;
m	:	$m_2 - m_1$;
m	:	a subscript denoting model;

p	:	a subscript denoting prototype;
R	:	model-prototype ratio;
S_s	:	specific storage (volume of water released from storage in a unit volume of the aquifer under a unit head decline);
t	:	time since an initial flow system;
v_x, v_y, v_z	:	rectangular components of the instantaneous bulk velocity in the medium;
V_x, V_y	:	instantaneous averages of v_x and v_y over thickness (z dimension) of the aquifer;
δh_1	:	amount of sudden change in water level;
$\phi(x,y,z,t)$	:	piezometric (hydraulic) head in the medium;
ν	:	K/S_s

REFERENCES CITED

Bear, J., Scales of viscous analogy models for ground-water studies, Proc. Amer. Soc. Civil Engrs., 86, HY 2, pp. 11-23, 1960

Dachler, R., Grundwasserströmung, Julius Springer, Vienna, 141 pp., 1936.

Dietz, D. N., Den modelproef ter bentudeering van niet-stationnaire bewegingen van het grondwater, Water, 25, The Hague, 1941.

Gunther, E., Lösung von Grundwasseraufgaben mit Hilfe der Strömung in dünnen Schichten, Wasserkraft und Wasserwirtschaft, 35, 1940.

Hantush, M. S., Flow of Ground Water in Sands of Nonuniform Thickness, Part 1. Flow in a Wedge-Shaped Aquifer, J. Geophys. Research, 67, pp. 703-709, 1962.

----------, Flow of Ground Water in Sands of Nonuniform Thickness, Part 2. Approximate Theory, J. Geophys. Research, 67, pp. 711-720, 1962.

----------, Hydraulics of Wells in Advances in Hydroscience, V. T. Chow, ed., Academic Press, New York, pp. 281-432, 1964.

Santing, G., Infiltratie en modelonderzoek, Water, 35, The Hague, 1951.

Todd, D. K., Unsteady flow in porous media by means of a Hele-Shaw viscous fluid model, Trans. Amer. Geophys. Union, 35, pp. 905-916, 1954.

----------, Ground Water Hydrology, John Wiley and Sons, New York, 336 pp., 1959.

This thesis is accepted on behalf of the faculty of the Institute by the following committee:

Gerard Wolfgang Groos.

Charles Holmes

William Rowe

A. T. Braddock

Date: April 23, 1965